

# When Does Context Help? Error Dynamics of Contextual Information in Large Language Models

Dingzirui Wang<sup>1</sup> Xuanliang Zhang<sup>1</sup> Keyan Xu<sup>1</sup> Qingfu Zhu<sup>1</sup> Wanxiang Che<sup>1</sup> Yang Deng<sup>2</sup>

## Abstract

Contextual information at inference time, such as demonstrations, retrieved knowledge, or interaction history, can substantially improve large language models (LLMs) without parameter updates, yet its theoretical role remains poorly understood beyond specific settings such as in-context learning (ICL). We present a unified theoretical framework for analyzing the effect of arbitrary contextual information in Transformer-based LLMs. Our analysis characterizes contextual influence through output error dynamics. In a single-layer Transformer, we prove that the context-conditioned error vector decomposes additively into the baseline error vector and a contextual correction vector. This yields necessary geometric conditions for error reduction: the contextual correction must align with the negative baseline error and satisfy a norm constraint. We further show that the contextual correction norm admits an explicit upper bound determined by context–query relevance and complementarity. These results extend to multi-context and multi-layer Transformers. Experiments across ICL, retrieval-augmented generation, and memory evolution validate our theory and motivate a principled context selection strategy that improves performance by 0.6%.

## 1. Introduction

Providing query-related **contextual information** in the input is an effective method to improve the inference performance of large language models (LLMs) without fine-tuning. This paradigm, broadly referred to as context engineering (Mei et al., 2025), now underpins a wide spectrum of methods, including In-Context Learning (ICL) via demonstrations (Dong et al., 2024), Retrieval-Augmented Generation (RAG) through external knowledge injection (Li et al.,

<sup>1</sup>Harbin Institute of Technology <sup>2</sup>Singapore Management University. Correspondence to: Dingzirui Wang <dzwang@ir.hit.edu.cn>, Wanxiang Che <car@ir.hit.edu.cn>.

2025), and Memory Evolution (ME) based on historical interactions (Luo et al., 2026). Despite their empirical success, these methods are often developed in isolation, guided by heuristic intuitions rather than a unified understanding of how contextual information influences inference.

Recent theoretical efforts have begun to probe the role of context, primarily focusing on the internal mechanisms of ICL (Huang et al., 2024; Zhang et al., 2024). These studies typically analyze idealized settings where contextual demonstrations and test queries are drawn from the same distribution or share a common functional relationship. Parallel work in RAG (Xu et al., 2025a) examines how statistical properties of retrieved knowledge, such as relevance or redundancy, affect downstream performance. While valuable, these analyses exhibit two fundamental limitations. (i) Existing theories are **tightly coupled to specific context types**, most notably ICL demonstrations, limiting their applicability to the broader ecosystem of context engineering methods. (ii) Most analyzes **rely on distributional alignment assumptions between context and query** that are routinely violated in practice, especially for memory-based or dynamically generated context. As a result, we currently lack a general theoretical principle that explains how arbitrary contextual information affects LLM inference.

To this end, we develop a unified theoretical framework for understanding the effect of arbitrary contextual information on Transformer-based LLMs (Vaswani et al., 2017) during inference. Rather than categorizing context by its source or semantics, we analyze its effect through the lens of output error dynamics. Our main conclusions are summarized in Table 1. We first show that, in the single-context and single-layer Transformer setting, **the context-conditioned error vector decomposes additively into the baseline error vector and a contextual correction vector**. Based on this, we derive the geometric conditions of the context to reduce error and prove that the norm of the contextual correction vector is inherently upper-bounded by the relevance and complementarity between the context and the user query. We then extend these conclusions to multi-context and multi-layer models, where we prove that analogous conclusions about context continue to hold in these settings.

We empirically validate our theory across three major con-

Table 1. The main findings and corresponding evidence of this paper.

Finding	Evidence	Experiment
<i>Additive error decomposition</i> : context-conditioned error vector equals baseline error vector plus contextual correction vector in Transformers	Theorem 2	§4.2
<i>Geometric condition for error reduction</i> : sufficient angular alignment between contextual correction and negative baseline error, relative to the ratio between their norms	Theorem 3	§4.2
<i>Upper bound on contextual correction norm</i> : governed by the relevance and complementarity between the contextual information and the user query	Theorem 3	§4.3

text engineering paradigms (ICL, RAG, and ME) using four mainstream LLMs and seven datasets spanning three tasks. Across all settings, experimental results closely match our theoretical predictions. Analysis of failure cases reveals a unifying explanation: ineffective contexts primarily arise from poor angular alignment with the baseline error or insufficient correction norms. Motivated by these insights, we introduce a simple context selection strategy based on angular alignment and norm upper bounds, achieving an average relative improvement of 0.6% over strong baselines, shedding light on future research. Together, our results provide a principled foundation for understanding and designing context engineering methods for LLMs.

Our contributions are as follows:

- We present a general theoretical framework that characterizes how arbitrary contextual information affects inference in Transformer models through output error dynamics.
- We derive the necessary geometric conditions of contextual information that reduce output error (i.e., the angle and norm of contextual correction vectors) and establish an upper bound on contextual correction determined by context–query relevance and complementarity.
- Through extensive experiments across ICL, RAG, and ME, four LLMs, and seven datasets, we empirically validate our theory and identify **angular misalignment and insufficient correction norms** as the dominant causes of ineffective contextual information, translating theory into practical context selection strategies.

## 2. Preliminary

In this section, we introduce some necessary mathematical notation. Following prior work (Zhang et al., 2024; Lu et al., 2025), we regard the contextual information, user input, and output as single semantic vectors after encoding them separately. In Appendix C.1, we discuss that our conclusions continue to hold when the inputs and outputs consist of multiple tokens. Specifically, let  $d \in \mathbb{N}$  denote the embedding dimension. We consider the input matrix  $E = [t, x] \in \mathbb{R}^{d \times 2}$ , where  $t \in \mathbb{R}^d$  represents the contextual information and  $x \in \mathbb{R}^d$  represents the user input. The prediction function  $f : \mathbb{R}^{L \times d} \rightarrow \mathbb{R}^{L \times d}$  maps

an input of arbitrary length  $L$  to an output of the same length. Given a target  $y \in \mathbb{R}^d$ , we view the output at the position corresponding to  $x$ , denoted  $f_x$ , as the model readout and define the **context-conditioned error vector**  $e(t, x) := f_x(t, x) - y \in \mathbb{R}^d$ . As a comparison, we define the **baseline error vector**  $e(x) := f_x(x) - y$ .

Following prior work (Zhang et al., 2024; Huang et al., 2024), we primarily focus on the Transformer architecture. Specifically, the model we consider consists of one or more Transformer blocks, where each block contains an attention layer and an MLP layer with a residual connection.

**Attention layer** Let  $W_Q, W_K, W_V, W_O \in \mathbb{R}^{d \times d}$  be the query matrix, key matrix, value matrix, and output projection matrix, respectively. For any vector  $z \in \mathbb{R}^d$ , define  $q_z := W_Q z, k_z := W_K z, v_z := W_V z$ . Define the query, key, and value matrices  $Q = [q_t, q_x] \in \mathbb{R}^{d \times 2}, K = [k_t, k_x] \in \mathbb{R}^{d \times 2}, V = [v_t, v_x] \in \mathbb{R}^{d \times 2}$ . Let the  $(i, j)$ -th entry of the score matrix  $S \in \mathbb{R}^{2 \times 2}$  be

$$S_{ij} := \frac{\langle q_{\bullet(i)}, k_{\bullet(j)} \rangle}{\sqrt{d}} \quad (i, j \in \{t, x\}),$$

and apply the softmax operation row-wise. Denote  $A := \text{softmax}(S) \in \mathbb{R}^{2 \times 2}$ . Then the attention output at position  $u \in \{t, x\}$  is defined as

$$\text{AttnOut}_u(E) := W_O \left( \sum_{w \in \{t, x\}} A_{uw} v_w \right) \in \mathbb{R}^d.$$

The attention layer with a residual connection at position  $u$  is

$$\text{Attn}_u(E) := E_{\bullet(u)} + \text{AttnOut}_u(E) \in \mathbb{R}^d.$$

**MLP layer** Given weights  $W_1, W_2 \in \mathbb{R}^{d \times d}$ . Let the nonlinear activation function  $\sigma : \mathbb{R}^d \rightarrow \mathbb{R}^d$  be 1-Lipschitz. We define the MLP layer with the residual connection by

$$\text{MLP}(z) := z + W_2 \sigma(W_1 z), \quad z \in \mathbb{R}^d.$$

Finally, the output of a single block is defined as

$$\text{Block}_u(E) := \text{MLP}(\text{Attn}_u(E)) \in \mathbb{R}^d.$$

In Appendix C.2, we discuss the impact of other architectural components of Transformers on our conclusions.

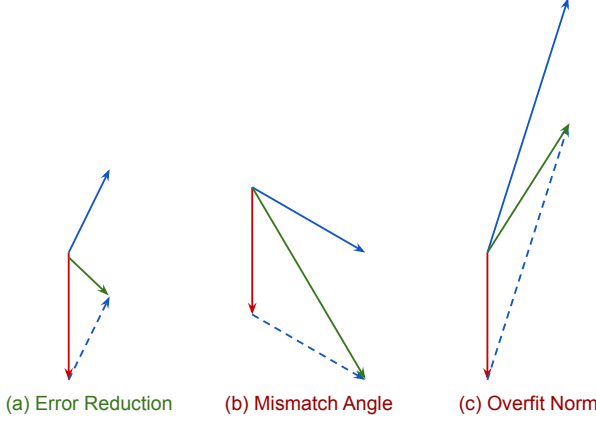


Figure 1. The illustration of how the contextual information affects the output error. The red vector denotes the baseline error vector  $e(x)$ , the blue vector denotes the contextual correction vector  $g(t, x)$ , and the green vector denotes the context-conditioned error vector  $e(t, x)$ . (a) the norm and direction of the contextual correction vector are appropriate, so the resulting error norm is smaller than the original error; (b) the norm of the contextual correction vector is appropriate, but its direction is not aligned with the negative direction of the error, which leads to a larger error; (c) the angle of the contextual correction vector is appropriate, but its norm is much larger than that of the original error, which also leads to a larger error. We present a case study in Appendix C.3.

### 3. Error Dynamics of Contextual Information

In this section, we study how contextual information affects the output error. We first show that for a single context on a single-layer Transformer, the context-conditioned error vector  $e(t, x)$  equals the sum of the baseline error vector  $e(x)$  and the contextual correction vector  $g(t, x)$ . Then we prove that, for multiple contexts and multi-layer models, the gain has a similar effect on the error. The proofs related to this section are deferred to Appendix A.

#### 3.1. Single Layer, Single Information

In this part, we discuss how a single piece of contextual information affects the output error in a single-layer Transformer. We first provide the definition of **contextual correction vector**. Then, we derive the condition under which contextual information helps reduce the output error, and we provide an upper bound for the norm of the vector.

We denote the attention weights at position  $x$  by  $\alpha_{x \leftarrow t} := A_{xt}$ ,  $\alpha_{x \leftarrow x} := A_{xx}$ . Let  $\delta_{\text{attn}}(t, x) = \text{Attn}_x([t, x]) - \text{Attn}_x([x])$  denote the change in the attention output. Let the Jacobian matrix of the MLP be:

$$J_{\text{MLP}}(z) := I + W_2 J_\sigma(W_1 z) W_1, \quad (1)$$

where  $\|J_\sigma(\cdot)\| \leq 1$  holds almost everywhere<sup>1</sup>. We then

<sup>1</sup>In this paper,  $\|\cdot\|$  denotes the Euclidean norm for vectors and the operator norm induced by the Euclidean norm for matrices

define the vector of the context information as follows:

**Definition 1** (Contextual Correction Vector).

$$g(t, x) := \int_0^1 J_{\text{MLP}}(\text{Attn}_x([x]) + s \delta_{\text{attn}}(t, x)) \delta_{\text{attn}}(t, x) ds$$

Definition 1 can be viewed as the change in the output caused by the context information after it sequentially passes through the attention and MLP layers, relative to the original input. Based on Definition 1, we have:

$$\text{Theorem 2. } e(t, x) = e(x) + g(t, x)$$

Theorem 2 shows that the context-conditioned error is the vector sum of the baseline error and the contextual correction. Considering that all three terms in Theorem 2 are vectors in  $\mathbb{R}^d$ , achieving  $|e(t, x)| < |e(x)|$  requires more than directional alignment alone: the contextual correction must not only point sufficiently toward the negative baseline error but also have a controlled magnitude, as illustrated in Figure 1. We formalize these geometric requirements of the contextual information as the following theorem.

**Theorem 3.** *For a single-layer Transformer with a single context, the contextual correction vector satisfies the following norm and direction conditions.*

Vector Norm. Let  $L_{\text{MLP}} := 1 + \|W_1\| \|W_2\|$ , we have  $\|g(t, x)\| \leq L_{\text{MLP}} \alpha_{x \leftarrow t} \|W_2\| \|v_t - v_x\|$

Vector Direction. If  $g(t, x) \neq 0$  and  $e(x) \neq 0$ , define

$$\rho(t, x) := \frac{\langle -e(x), g(t, x) \rangle}{\|e(x)\| \|g(t, x)\|} \in [-1, 1]$$

Then, if introducing the new information reduces the error, i.e., if  $\|e(t, x)\| < \|e(x)\|$ , we must have

$$\rho(t, x) > \frac{\|g(t, x)\|}{2 \|e(x)\|}$$

$\rho(t, x)$  of Theorem 3 is the cosine value of the angle between the contextual correction vector and the negative baseline error. We refer to  $\rho(t, x)$  as the **context-error angle**. Intuitively, Theorem 3 requires that the context-error angle not be too small, i.e., the contextual correction vector should align as closely as possible with the negative direction of the baseline error vector. Simultaneously, the norm of the contextual correction vector must not be excessively large, as this would cause the model to over-attend to the contextual correction vector and ignore the user query.

Besides the condition required for contextual information to reduce error, Theorem 3 also provides an upper bound on the norm of the contextual correction vector. For a fixed model, this upper bound is mainly determined by two factors: (i) *relevance*  $\alpha_{x \leftarrow t}$ : the attention weight that the context receives from the user input; (ii) *complementarity*  $\|v_t - v_x\|$ : the complementarity between the context and the user query in the projection space induced by  $W_V$ .

### 3.2. Single Layer, Multiple Context

Considering that a single context could not fully cover the content needed for the user query, most approaches include multiple pieces of context in the input. Therefore, in this part, we discuss the effect of introducing a new piece of context on the error when some context already exists. Let the existing context set be  $T = \{t_1, \dots, t_n\}$  and the new context be  $t_{n+1}$ . We can derive that:

**Corollary 4.** *Let*

$$\bar{v}_T := \sum_{i=1}^n \alpha_{x \leftarrow t_i} v_{t_i} + \alpha_{x \leftarrow x} v_x.$$

*Then the conclusion of Theorem 3 still holds after replacing  $v_x$  with  $\bar{v}_T$  and  $t$  with  $t_{n+1}$ .*

Compared with Theorem 3, Corollary 4 shows that the multi-context case can be viewed as treating the existing context and the user query as a whole, using it as the effective user input. Each existing piece of context is weighted by its attention coefficient to the user query.

### 3.3. Multi Layer, Single Context

In this part, we discuss how context functions in a multi-layer Transformer. Consider a Transformer with  $L$  layers. Denote the hidden states at layer  $\ell$  by

$$H^{(\ell)}(t, x) = [h_u^{(\ell)}(t, x)]_{u \in \{t, x\}}, \quad \ell = 0, 1, \dots, L,$$

where  $H^{(0)}(t, x)$  is the input embedding. The update of layer  $\ell$  at position  $x$  is given by

$$\tilde{h}_x^{(\ell)}(t, x) := h_x^{(\ell-1)}(t, x) + \text{Attn}_x^{(\ell)}(H^{(\ell-1)}(t, x)),$$

$$h_x^{(\ell)}(t, x) := \tilde{h}_x^{(\ell)}(t, x) + \text{MLP}^{(\ell)}(\tilde{h}_x^{(\ell)}(t, x)).$$

The overall model output at position  $x$  is denoted by  $f_x^{(L)}(t, x) := h_x^{(L)}(t, x)$ , and we define  $e^{(L)}(t, x) := f_x^{(L)}(t, x) - y$  and  $e^{(L)}(x) := f_x^{(L)}(x) - y$ .

For layer  $\ell$ , the layer of the attention output at position  $x$  is

$$\begin{aligned} \delta_{\text{attn}}^{(\ell)}(t, x) &:= \text{Attn}_x^{(\ell)}([t, x]) - \text{Attn}_x^{(\ell)}([x]) \\ &= \alpha_{x \leftarrow t}^{(\ell)} W_O^{(\ell)} \Delta v^{(\ell)}, \end{aligned}$$

where  $\Delta v^{(\ell)} := v_t^{(\ell)} - v_x^{(\ell)}$ , and  $\alpha_{x \leftarrow t}^{(\ell)}$  is the attention weight of position  $x$  on  $t$  at layer  $\ell$ .

In analogy to Definition 1, we define the contextual correction vector at layer  $\ell$  as  $g^{(\ell)}(t, x)$  by

$$\int_0^1 J_{\text{MLP}^{(\ell)}}(\text{Attn}_x^{(\ell)}([x]) + s \delta_{\text{attn}}^{(\ell)}(t, x)) \delta_{\text{attn}}^{(\ell)}(t, x) ds$$

Let the mapping composed of layers  $\ell + 1$  to  $L$  be

$$\Phi^{(\ell+1:L)}(z) := f^{(L)} \circ \dots \circ f^{(\ell+1)}(z).$$

Following Definition 1, the local vector  $g^{(\ell)}(t, x)$  at layer  $\ell$ , after being propagated through the upper layers, yields an amplified vector in the output space:

$$\tilde{g}^{(\ell)}(t, x) := \int_0^1 J_{\Phi^{(\ell+1:L)}}(h_x^{(\ell)}(x) + s g^{(\ell)}(t, x)) g^{(\ell)}(t, x) ds$$

Due to the residual connections, we define the overall contextual correction vector as  $g^{(L)}(t, x) := \sum_{\ell=1}^L \tilde{g}^{(\ell)}(t, x)$ . It can be derived that

$$e^{(L)}(t, x) = e^{(L)}(x) + g^{(L)}(t, x),$$

and hence, we obtain:

**Corollary 5.** *In a multi-layer Transformer, the contextual correction vector satisfies the following norm and direction conditions.*

**Vector Norm.** *Let  $L_{\text{MLP}}^{(\ell)} := 1 + \|W_1^{(\ell)}\| \|W_2^{(\ell)}\|$ , we have*

$$\begin{aligned} \|g^{(L)}(t, x)\| &\leq \\ &\sum_{\ell=1}^L \left( \prod_{j=\ell+1}^L L_{\text{blk}}^{(j)} \right) L_{\text{MLP}}^{(\ell)} \alpha_{x \leftarrow t}^{(\ell)} \|W_O^{(\ell)}\| \|v_t^{(\ell)} - v_x^{(\ell)}\|. \end{aligned}$$

**Vector Direction.** *If  $\|g^{(L)}(t, x)\| > 0$  and  $e^{(L)}(x) \neq 0$ , define*

$$\rho^{(L)}(t, x) := \frac{\langle -e^{(L)}(x), g^{(L)}(t, x) \rangle}{\|e^{(L)}(x)\| \|g^{(L)}(t, x)\|} \in [-1, 1]$$

*Then, if introducing the new information reduces the error, i.e., if  $\|e^{(L)}(t, x)\| < \|e^{(L)}(x)\|$ , we must have*

$$\rho^{(L)}(t, x) > \frac{\|g^{(L)}(t, x)\|}{2 \|e^{(L)}(x)\|}$$

The definitions of  $W_1^{(\ell)}$  and  $W_2^{(\ell)}$  are the same as Equation 1. From Corollary 5, we can see that for the upper bound of the vector norm, each layer produces a local vector  $g^{(\ell)}$ , whose norm is still jointly determined by the relevance ( $\alpha_{x \leftarrow t}^{(\ell)}$ ) and the complementarity ( $\|v_t^{(\ell)} - v_x^{(\ell)}\|$ ) of the corresponding layer. The upper layers scale or amplify the vector from the lower layers through their Lipschitz constants  $\prod_{j=\ell+1}^L L_{\text{blk}}^{(j)}$ . If the Lipschitz constants are smaller than 1, i.e., the model is stable to input perturbations, then increasing the number of layers shrinks the vector brought by the contextual information, and vice versa.

## 4. Experiment

In this section, we empirically validate the three conclusions about contextual information: (i) how the contextual correction vector affects the error (§4.2); (ii) how relevance and complementarity affect the norm of the contextual correction vector (§4.3); (iii) how multi-context and multi-layer affect the above conclusion (§4.4).

#### 4.1. Experiment Setup

**Dataset** We mainly conduct experiments on three types of mainstream tasks to validate our theoretical conclusions, which include: (i) Math: MATH (Hendrycks et al., 2021), CHAMP (Mao et al., 2024); (ii) Reason: TheoremQA (Chen et al., 2023), MMLU-Redux (Gema et al., 2025), GPQA (Rein et al., 2024); (iii) QA: NaturalQuestions (Kwiatkowski et al., 2019), FinQA (Chen et al., 2021). We introduce these datasets in detail in Appendix B.1.

**Model** We conduct experiments on four mainstream LLMs, including Llama-3.1-8B-Instruct (Llama-3.1-8B) (Grattafiori et al., 2024), DeepSeek-R1-Distill-Llama-8B (Llama-R1-8B) (DeepSeek-AI et al., 2025), Qwen3-8B (Yang et al., 2025), and Minstral-8B-Instruct-2410 (Minstral-8B) (Mistral AI team, 2024). Given that these LLMs cover different families, we believe they can adequately validate our theoretical conclusions.

**Setup** We first filter the bad cases under the no-context setting, ensuring that the experimental data consist of queries that the models cannot solve on their own. To reflect mainstream ways of leveraging context, we construct contextual information as follows: (i) ICL: we use demonstrations from the training set as context; (ii) RAG: we use the knowledge provided in the dataset as context; (iii) ME: at test time, we use historical test instances as context. The detailed methodological design and experimental configurations are provided in Appendix B.2, and the computation of various parameters is detailed in Appendix B.3. **We merge the data from all datasets, models, and methods as our experimental data.** To uniformly reflect the relationship, we normalize the results of all settings. All our experiments are running on two H100-80G and are based on Transformers (Wolf et al., 2020) and vLLM (Kwon et al., 2023).

#### 4.2. Effect of Contextual Correction Vector on Error

In this part, we validate the conclusion in Theorem 3 that the error reduction achieved by introducing contextual information depends on the contextual correction vector. We first analyze how the norm and direction of the contextual correction vector affect the error reduction, where the experimental results are shown in Figure 2, from which we can observe that: (i) Almost all data points with decreased error are concentrated in the region where  $\frac{\|g(t,x)\|}{2\|e(x)\|} < \rho(t,x)$ , which empirically validates our findings on error reduction in Theorem 3. (ii) There are many points with increased error around  $\rho(t,x) = 1$ ,  $\frac{\|g(t,x)\|}{2\|e(x)\|} = 1$ , indicating that for data whose direction is well aligned with the negative error direction, an excessively large norm causes the model to over-emphasize the contextual information while neglecting the user query, leading to significant increases in error.

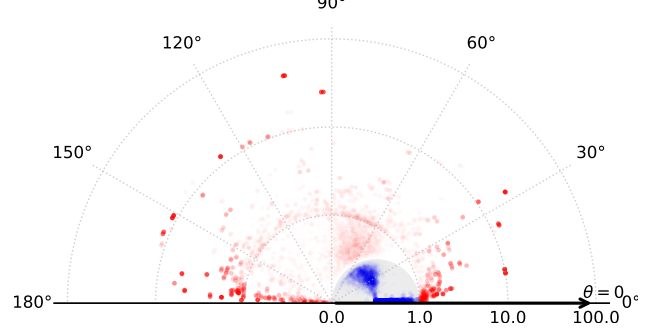


Figure 2. The variation of error change  $\|e(t, x) - e(x)\|$  with respect to the contextual correction vector  $g(t, x)$ , where each point represents one data instance. The length of the vector from the axis origin to each point represents  $\frac{\|g(t,x)\|}{2\|e(x)\|}$ , and the angle with the positive  $x$ -axis represents  $\arccos \rho(t, x)$  (i.e., the angle between the contextual correction vector and the negative baseline error vector). Blue and red indicate that the error change is smaller or larger than 0, respectively, and darker colors indicate larger absolute values. The gray region corresponds to  $\frac{\|g(t,x)\|}{2\|e(x)\|} < \rho(t, x)$ .

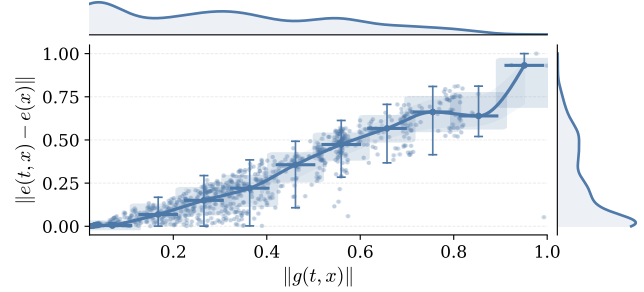


Figure 3. The variation of error change norm  $\|e(t, x) - e(x)\|$  with respect to the contextual correction vector norm  $\|g(t, x)\|$ , where each point represents one data instance. The curves at the top and to the right show the distributions of the data points along the  $x$ -axis and  $y$ -axis, respectively. The Pearson correlation coefficient for the fitted points is 0.903.

In addition, we analyze how error change varies with the contextual correction vector, which is shown in Figure 3. From the figure, we can see that the error change exhibits an overall positive correlation with the norm of the contextual correction vector, which corroborates the quantitative relationship between them in Theorem 3. Also, we can observe a slight kink around  $\|g(t, x)\| \approx 0.9$  on the plot. Judging from the point density, this is likely due to the smaller number of samples in this region.

#### 4.3. Effect of Contextual Complementarity and Relevance on Contextual Correction Vector

In this part, we validate the conclusion in Theorem 3 regarding how different factors affect the upper bound of the contextual correction vector. We compute how the contextual correction vector varies with relevance ( $\alpha_{x \leftarrow t}$ ) and complementarity ( $\|v_t - v_x\|$ ). The experimental results are

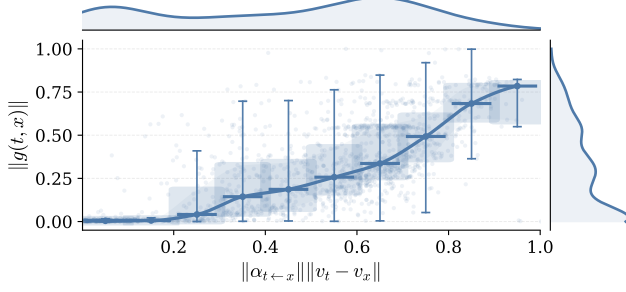


Figure 4. The variation of contextual correction vector norm  $\|g(t, x)\|$  with respect to the relevance and complementarity  $\alpha_{x-t} \|v_t - v_x\|$ , where each point represents one data instance. The curves at the top and to the right show the distributions of the data points along the  $x$ -axis and  $y$ -axis, respectively. The Pearson correlation coefficient for the fitted points is 0.770.

shown in Figure 4. From the figure, we can see that: (i) The norm of the contextual correction vector is overall positively correlated with  $\alpha_{x-t} \|v_t - v_x\|$ , which verifies the quantitative relationship of the vector with relevance and complementarity in Theorem 3. (ii) Overall, the relationship between relevance, complementarity, and the vector norm is not strictly linear since Theorem 3 only provides an upper bound for the vector norm that depends on relevance and complementarity. In practice, the vector norm in our experiments is often smaller than this upper bound, so the overall relationship is not strictly linear. (iii) From the data distribution, most samples have their relevance and complementarity concentrated in the top 50%, whereas the vector norm is mostly below 0.1. This suggests that even for contexts with relatively strong relevance, the model does not fully exploit them, which limits its performance.

#### 4.4. Effect of Contextual Correction Vector under the Multi-Context and Multi-Layer setting

In this part, we validate the conclusions stated in Corollary 4 and Corollary 5 under the multi-context and multi-layer settings. For the multi-context setting, we increase the number of input contexts from 1 to 5. For the multi-layer setting, we collect the computed results from different layers of the model. Due to space limitations, we report only the overall trend of the data, where we partition the points along the x-axis into ten equal bins based on the number of points and plot the median value within each bin. We also discuss the change of  $g(t, x)$  across different context numbers in Appendix D.4 and different layers in Appendix D.3.

The results are shown in Figure 5 and Figure 6. We provide the complete experimental results in Appendix D.1. From the results, we observe that: (i) Across all settings, the plots show an overall increasing trend, which supports the conclusions in Corollary 4 and Corollary 5. (ii) Overall, the values under multi-context are larger than those under multi-

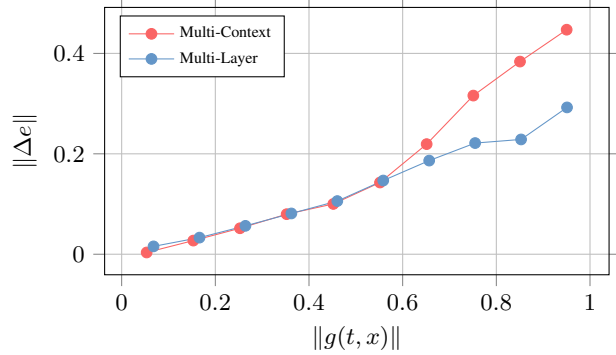


Figure 5. The variation of error change norm with respect to the contextual correction vector norm  $\|g(t, x)\|$  under the **multi-context** and **multi-layer** settings, where  $\Delta e$  denotes  $e(T, x|t_{n+1}) - e(T, x)$  (multi-context) or  $e^{(L)}(t, x) - e^{(L)}(x)$  (multi-layer), and each point represents one data instance. The curves at the top and to the right show the distributions of the data points along the  $x$ -axis and  $y$ -axis, respectively.

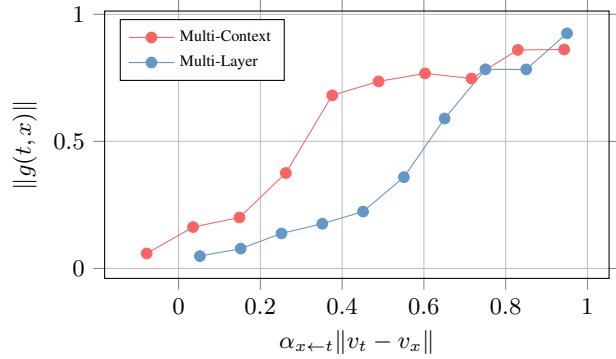


Figure 6. The variation of contextual correction vector norm  $\|g(t, x)\|$  with respect to the relevance  $\alpha_{x-t}$  and complementarity  $\|v_t - v_x\|$  under the **multi-context** and **multi-layer** settings, where each point represents one data instance. The curves at the top and to the right show the distributions of the data points along the  $x$ -axis and  $y$ -axis, respectively.

layer. This is because, due to the residual stream, the effect of  $\|g(t, x)\|$  at the current layer is diluted by information from previous layers under the multi-layer setting, thereby reducing its impact on the output error.

## 5. Theory-Guided Context Selection

In this section, we examine how the theoretical insights developed in this work can be leveraged to improve context selection in practical LLM inference. Our objective is not to introduce new state-of-the-art methods but to validate the predictive power of our theoretical analysis and demonstrate how it can inform principled design choices in real-world settings. Accordingly, we focus on lightweight, theory-guided enhancements on Llama-3.1-8B and Qwen3-8B that incur minimal additional computational overhead.

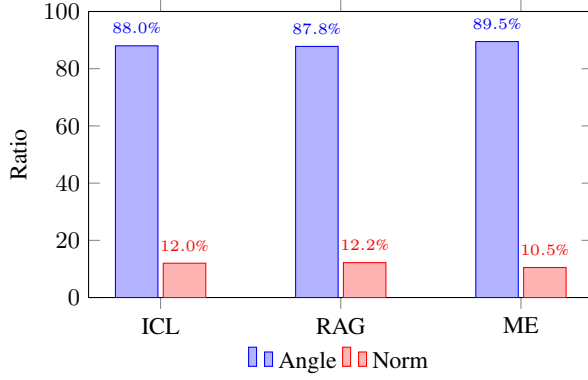


Figure 7. Distribution of error types of example where the context-conditioned error vector is greater than the baseline error vector. Angle indicates that the direction of the vector is misaligned and Norm indicates that the norm of the vector is too large.

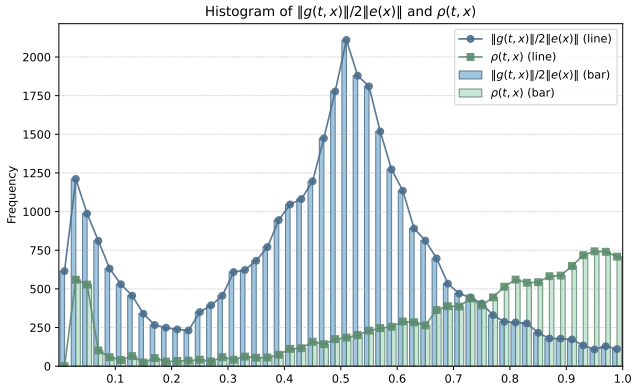


Figure 8. Distribution of the vector norm  $\|g(t, x)\|/2\|e(t, x)\|$  and the vector angle  $\rho(t, x)$  on examples where the error decreases.

### 5.1. Error Type Distribution

To investigate the main causes of errors, we divide the current bad cases into two categories: (i)  $\frac{\|g(t, x)\|}{2\|e(t, x)\|} > \rho(t, x)$ : the model over-attends to the contextual information; (ii)  $\rho(t, x) < 0$ : the contextual information is irrelevant to the original error. The experimental results are shown in Figure 7, from which we can see that the dominant error type is still caused by the misalignment between the directions of the vector and the error. We also compute the distributions of  $\|g(t, x)\|/2\|e(t, x)\|$  and  $\rho(t, x)$  on examples where the error decreases, as shown in Figure 8. From the figure, we observe that  $\rho(t, x)$  is overall skewed toward 1, indicating that contextual vector is already well aligned with the negative direction of the original error. However, most values of  $\|g(t, x)\|/2\|e(t, x)\|$  lie around 0.1 to 0.5, which suggests that even for these examples, the vector norm is still insufficient to completely eliminate the error.

Based on the above analysis, we argue that improvements in context usage should proceed from two aspects: (i) ensuring that the direction of the context vector is aligned

Table 2. Performance of ICL with top-1 selection. Zero denotes inference without contextual information. The best performance under each setting is marked in **bold**.

Model	Method	MATH	GPQA	FinQA
Llama-3.1-8B	Zero	46.0	31.3	48.6
	BM25	46.8	42.4	49.2
	DICL (Kapuriya et al., 2025)	47.4	43.0	51.3
	GenICL (Zhang et al., 2025)	47.6	43.0	<b>51.6</b>
	TopicK (Kweon et al., 2025)	47.0	42.9	49.8
	<b>Ours</b>	<b>48.0</b>	<b>43.4</b>	51.1
Qwen3-8B	Zero	87.0	64.6	60.1
	BM25	88.0	63.6	64.2
	DICL (Kapuriya et al., 2025)	88.0	64.6	67.1
	GenICL (Zhang et al., 2025)	88.4	65.2	<b>67.3</b>
	TopicK (Kweon et al., 2025)	86.2	64.1	64.2
	<b>Ours</b>	<b>89.2</b>	<b>65.7</b>	66.7

Table 3. Performance of RAG with top-1 selection. Zero denotes inference without contextual information. TQA denotes TheoremQA and NQ denotes NaturalQuestions. InstructRAG refers to the InstructRAG-ICL (Wei et al., 2025b).

Model	Method	CHAMP	TQA	NQ
Llama-3.1-8B	Zero	14.1	26.8	38.5
	BM25	22.2	37.6	74.7
	DPR (Karpukhin et al., 2020)	23.0	38.4	75.6
	InstructRAG (Wei et al., 2025b)	24.1	39.2	76.3
	ReFeedL (Yun et al., 2025)	24.8	40.0	<b>77.1</b>
	<b>Ours</b>	<b>25.2</b>	<b>40.8</b>	76.8
Qwen3-8B	Zero	39.6	54.6	44.2
	BM25	42.6	62.8	73.8
	DPR (Karpukhin et al., 2020)	43.7	63.6	74.5
	InstructRAG (Wei et al., 2025b)	44.8	64.4	75.1
	ReFeedL (Yun et al., 2025)	<b>45.2</b>	65.1	75.6
	<b>Ours</b>	<b>45.2</b>	<b>66.3</b>	<b>76.9</b>

with the negative direction of the error so that the provided information can indeed reduce the error; (ii) increasing the contextual correction vector norm by enhancing relevance and complementarity, thereby further reducing the error.

### 5.2. Context Selection Strategies

We introduce two strategies to improve context selection: aligning vector direction and increasing vector norm.

**Vector Direction** Since computing the angle  $\rho(t, x)$  in Theorem 3 depends on the ground-truth answer, we cannot estimate this angle directly. Following prior works (Xie et al., 2023; Liu et al., 2025), we use a smaller model to predict this angle. Specifically, we take ELECTRA-Large-Discriminator (Clark et al., 2020) as the predictor and merge the training splits of each dataset as the training data. The inputs consist of the user query, the context, and the prediction of the LLM without context, while the output is the corresponding  $\rho(t, x)$ . We report the relative error of the trained predictor in Appendix D.5.

Table 4. Performance of ME with top-1 selection. Zero denotes inference without contextual information. TQA denotes TheoremQA, MMLU denotes MMLU-Redux, and NQ denotes NaturalQuestions.

Model	Method	MATH	CHAMP	TQA	MMLU	GPQA	NQ	FinQA
Llama-3.1-8B	Zero	46.0	14.1	26.8	63.8	31.3	38.5	48.6
	BM25	46.4	14.4	27.0	64.1	31.8	38.9	49.0
	DC (Suzgun et al., 2025)	47.0	14.8	27.6	64.6	32.3	39.3	49.5
	ExpRAG (Wei et al., 2025a)	47.0	14.8	27.6	64.7	31.8	39.4	49.7
	ReMem (Wei et al., 2025a)	47.2	<b>15.2</b>	27.7	64.9	32.3	<b>39.8</b>	49.6
	<b>Ours</b>	<b>47.4</b>	<b>15.2</b>	<b>28.0</b>	<b>65.0</b>	<b>32.8</b>	39.7	<b>50.0</b>
Qwen3-8B	Zero	87.0	39.6	54.6	65.8	64.6	44.2	60.1
	BM25	87.2	40.0	54.8	66.0	65.2	44.6	60.4
	DC (Suzgun et al., 2025)	88.0	40.4	55.4	66.5	65.2	45.0	60.9
	ExpRAG (Wei et al., 2025a)	88.0	40.7	55.6	66.6	<b>65.7</b>	45.1	61.1
	ReMem (Wei et al., 2025a)	88.2	40.7	55.6	66.8	65.2	45.3	<b>61.5</b>
	<b>Ours</b>	<b>88.4</b>	<b>41.1</b>	<b>56.0</b>	<b>66.9</b>	<b>65.7</b>	<b>45.5</b>	61.4

**Vector Norm** According to Theorem 3, the upper bound of  $\|g(t, x)\|$  is determined by  $\alpha_{x \leftarrow t} \|v_t - v_x\|$ . Since  $\alpha_{x \leftarrow t}, v_t, v_x$  can be directly extracted, we feed the user query and the context into the LLM and directly extract the corresponding quantities from the model as  $\|g(t, x)\|$ .

To reduce computational costs, for each user input, we first use the method described in Appendix B.2 to coarsely select 32 candidate context passages. We then compute  $\rho(t, x)$  and  $\alpha_{x \leftarrow t} \|v_t - v_x\|$  for these candidates, select all contexts with  $\rho(t, x) < 1$ , and finally choose the context with the largest  $\alpha_{x \leftarrow t} \|v_t - v_x\|$  to guide LLM inference. To verify the effectiveness of the above strategy, we conduct experiments under different settings in Table 2, Table 3 and Table 4, where all settings employ the top-1 context during inference. From the tables, we can observe that compared with the baselines under each setting, our method achieves comparable or even better performance, leading to 0.6% relative improvement on average. Such results demonstrate the effectiveness of the proposed approach, thereby supporting the correctness and practical applicability of our conclusions.

## 6. Related Works

LLMs can benefit from contextual information at inference time (Mei et al., 2025). To understand how LLMs interpret context and to guide future improvements, many studies investigate context related mechanisms (Zhou et al., 2024). For ICL, many works take a bottom up approach. They start from theory and, under the assumption that the provided context and the user query are drawn from the same distribution, they prove convergence results showing that ICL can solve arbitrary tasks (Zhang et al., 2024; Mahankali et al., 2024; Li et al., 2024; Yang et al., 2024). Many other works take a top down approach. They analyze the origins of ICL capability and how context guides inference by examining the dynamics during training and inference (Park et al., 2025; Nguyen & Reddy, 2025; Smart et al., 2025). For RAG,

instead of analyzing based on a mathematical foundation, existing studies mainly focus on inference. They partition contexts by their effectiveness and observe RAG behavior under different effectiveness conditions to understand its mechanism (Ghosh et al., 2024; Joren et al., 2025; Xu et al., 2025a). For ME, mechanistic research is relatively limited. Current studies primarily focus on improving performance by managing and selecting effective memory (Suzgun et al., 2025; Wei et al., 2025a; Xu et al., 2025b).

These existing works suggest that most context related mechanistic studies are task specific and lack a unified explanatory theory. This limits our understanding of context and also makes it difficult to generalize to new context engineering methods in the future. To address this issue, we propose a unified framework for analyzing context. We introduce the contextual correction vector to measure context effectiveness, and we derive the geometric conditions that must hold when the context is effective.

## 7. Conclusion

In this paper, we propose a unified theory to explain how context works. We introduce the contextual correction vector to model the effectiveness of context and prove that the context-conditioned error vector equals the vector sum of the contextual correction vector and the baseline error vector. Building on this, we derive the geometric conditions under which context leads to error reduction and provide an upper bound on the norm of the contextual correction vector. We then show that similar conclusions continue to hold under multi-context and multi-layer settings. We conduct experiments across three methods (ICL, RAG, and ME), four LLMs, and seven datasets spanning three mainstream tasks, and the results are consistent with our theoretical predictions. Finally, we further analyze the current bad cases and find that the primary causes are angle misalignment and small vector norms, which can guide future improvements.

## References

Chen, W., Yin, M., Ku, M., Lu, P., Wan, Y., Ma, X., Xu, J., Wang, X., and Xia, T. TheoremQA: A theorem-driven question answering dataset. In Bouamor, H., Pino, J., and Bali, K. (eds.), *Proceedings of the 2023 Conference on Empirical Methods in Natural Language Processing*, pp. 7889–7901, Singapore, December 2023. Association for Computational Linguistics. doi: 10.18653/v1/2023.emnlp-main.489. URL <https://aclanthology.org/2023.emnlp-main.489/>.

Chen, Z., Chen, W., Smiley, C., Shah, S., Borova, I., Langdon, D., Moussa, R., Beane, M., Huang, T.-H., Routledge, B., and Wang, W. Y. FinQA: A dataset of numerical reasoning over financial data. In Moens, M.-F., Huang, X., Specia, L., and Yih, S. W.-t. (eds.), *Proceedings of the 2021 Conference on Empirical Methods in Natural Language Processing*, pp. 3697–3711, Online and Punta Cana, Dominican Republic, November 2021. Association for Computational Linguistics. doi: 10.18653/v1/2021.emnlp-main.300. URL <https://aclanthology.org/2021.emnlp-main.300/>.

Clark, K., Luong, M.-T., Le, Q. V., and Manning, C. D. Elec-trा: Pre-training text encoders as discriminators rather than generators. In *International Conference on Learning Representations*, 2020. URL <https://openreview.net/forum?id=r1xMH1BtvB>.

DeepSeek-AI, Guo, D., Yang, D., Zhang, H., Song, J., Zhang, R., Xu, R., Zhu, Q., Ma, S., Wang, P., Bi, X., Zhang, X., Yu, X., Wu, Y., Wu, Z. F., Gou, Z., Shao, Z., Li, Z., Gao, Z., Liu, A., Xue, B., Wang, B., Wu, B., Feng, B., Lu, C., Zhao, C., Deng, C., Zhang, C., Ruan, C., Dai, D., Chen, D., Ji, D., Li, E., Lin, F., Dai, F., Luo, F., Hao, G., Chen, G., Li, G., Zhang, H., Bao, H., Xu, H., Wang, H., Ding, H., Xin, H., Gao, H., Qu, H., Li, H., Guo, J., Li, J., Wang, J., Chen, J., Yuan, J., Qiu, J., Li, J., Cai, J. L., Ni, J., Liang, J., Chen, J., Dong, K., Hu, K., Gao, K., Guan, K., Huang, K., Yu, K., Wang, L., Zhang, L., Zhao, L., Wang, L., Zhang, L., Xu, L., Xia, L., Zhang, M., Zhang, M., Tang, M., Li, M., Wang, M., Li, M., Tian, N., Huang, P., Zhang, P., Wang, Q., Chen, Q., Du, Q., Ge, R., Zhang, R., Pan, R., Wang, R., Chen, R. J., Jin, R. L., Chen, R., Lu, S., Zhou, S., Chen, S., Ye, S., Wang, S., Yu, S., Zhou, S., Pan, S., Li, S. S., Zhou, S., Wu, S., Ye, S., Yun, T., Pei, T., Sun, T., Wang, T., Zeng, W., Zhao, W., Liu, W., Liang, W., Gao, W., Yu, W., Zhang, W., Xiao, W. L., An, W., Liu, X., Wang, X., Chen, X., Nie, X., Cheng, X., Liu, X., Xie, X., Liu, X., Yang, X., Li, X., Su, X., Lin, X., Li, X. Q., Jin, X., Shen, X., Chen, X., Sun, X., Wang, X., Song, X., Zhou, X., Wang, X., Shan, X., Li, Y. K., Wang, Y. Q., Wei, Y. X., Zhang, Y., Xu, Y., Li, Y., Zhao, Y., Sun, Y., Wang, Y., Yu, Y., Zhang, Y., Shi, Y., Xiong, Y., He, Y., Piao, Y., Wang, Y., Tan, Y., Ma, Y., Liu, Y., Guo, Y., Ou, Y., Wang, Y., Gong, Y., Zou, Y., He, Y., Xiong, Y., Luo, Y., You, Y., Liu, Y., Zhou, Y., Zhu, Y. X., Xu, Y., Huang, Y., Li, Y., Zheng, Y., Zhu, Y., Ma, Y., Tang, Y., Zha, Y., Yan, Y., Ren, Z. Z., Ren, Z., Sha, Z., Fu, Z., Xu, Z., Xie, Z., Zhang, Z., Hao, Z., Ma, Z., Yan, Z., Wu, Z., Gu, Z., Zhu, Z., Liu, Z., Li, Z., Xie, Z., Song, Z., Pan, Z., Huang, Z., Xu, Z., Zhang, Z., and Zhang, Z. Deepseek-r1: Incentivizing reasoning capability in llms via reinforcement learning, 2025. URL <https://arxiv.org/abs/2501.12948>.

Dong, Q., Li, L., Dai, D., Zheng, C., Ma, J., Li, R., Xia, H., Xu, J., Wu, Z., Chang, B., Sun, X., Li, L., and Sui, Z. A survey on in-context learning. In Al-Onaizan, Y., Bansal, M., and Chen, Y.-N. (eds.), *Proceedings of the 2024 Conference on Empirical Methods in Natural Language Processing*, pp. 1107–1128, Miami, Florida, USA, November 2024. Association for Computational Linguistics. doi: 10.18653/v1/2024.emnlp-main.64. URL <https://aclanthology.org/2024.emnlp-main.64/>.

Gema, A. P., Leang, J. O. J., Hong, G., Devoto, A., Mancino, A. C. M., Saxena, R., He, X., Zhao, Y., Du, X., Ghasemi Madani, M. R., Barale, C., McHardy, R., Harris, J., Kaddour, J., Van Krieken, E., and Minderlini, P. Are we done with MMLU? In Chiruzzo, L., Ritter, A., and Wang, L. (eds.), *Proceedings of the 2025 Conference of the Nations of the Americas Chapter of the Association for Computational Linguistics: Human Language Technologies (Volume 1: Long Papers)*, pp. 5069–5096, Albuquerque, New Mexico, April 2025. Association for Computational Linguistics. ISBN 979-8-89176-189-6. doi: 10.18653/v1/2025.nacl-long.262. URL [https://aclanthology.org/2025.nacl-long.262/](https://aclanthology.org/2025.nacl-long.262).

Ghosh, R., Seetharaman, R., Wadhwa, H., Aggarwal, S., Basu, S., Srinivasan, S., Zhao, W., Chaudhari, S., and Aghazadeh, E. Quantifying reliance on external information over parametric knowledge during retrieval augmented generation (RAG) using mechanistic analysis. In *The 7th BlackboxNLP Workshop*, 2024. URL <https://openreview.net/forum?id=PCi5h5PJNw>.

Grattafiori, A., Dubey, A., Jauhri, A., Pandey, A., Kadian, A., Al-Dahle, A., Letman, A., Mathur, A., Schelten, A., Vaughan, A., Yang, A., Fan, A., Goyal, A., Hartshorn, A., Yang, A., Mitra, A., Sravankumar, A., Korenev, A., Hinsvark, A., Rao, A., Zhang, A., Rodriguez, A., Gregerson, A., Spataru, A., Roziere, B., Biron, B., Tang, B., Chern, B., Caucheteux, C., Nayak, C., Bi, C., Marra, C., McConnell, C., Keller, C., Touret, C., Wu, C., Wong, C., Ferrer, C. C., Nikolaidis, C., Allonsius, D., Song, D., Pintz, D., Livshits, D., Wyatt, D., Esiobu, D., Choudhary, D., Mahajan, D., Garcia-Olano, D., Perino, D., Hupkes, D., Lakomkin, E., AlBadawy, E., Lobanova, E., Dinan,

E., Smith, E. M., Radenovic, F., Guzmán, F., Zhang, F., Synnaeve, G., Lee, G., Anderson, G. L., Thattai, G., Nail, G., Mialon, G., Pang, G., Cucurell, G., Nguyen, H., Kovala, H., Xu, H., Touvron, H., Zarov, I., Ibarra, I. A., Kloumann, I., Misra, I., Evtimov, I., Zhang, J., Copet, J., Lee, J., Geffert, J., Vranes, J., Park, J., Mahadeokar, J., Shah, J., van der Linde, J., Billock, J., Hong, J., Lee, J., Fu, J., Chi, J., Huang, J., Liu, J., Wang, J., Yu, J., Bitton, J., Spisak, J., Park, J., Rocca, J., Johnstun, J., Saxe, J., Jia, J., Alwala, K. V., Prasad, K., Upasani, K., Plawiak, K., Li, K., Heafield, K., Stone, K., El-Arini, K., Iyer, K., Malik, K., Chiu, K., Bhalla, K., Lakhotia, K., Rantala-Yeary, L., van der Maaten, L., Chen, L., Tan, L., Jenkins, L., Martin, L., Madaan, L., Malo, L., Blecher, L., Landzaat, L., de Oliveira, L., Muzzi, M., Pasupuleti, M., Singh, M., Paluri, M., Kardas, M., Tsimpoukelli, M., Oldham, M., Rita, M., Pavlova, M., Kambadur, M., Lewis, M., Si, M., Singh, M. K., Hassan, M., Goyal, N., Torabi, N., Bashlykov, N., Bogoychev, N., Chatterji, N., Zhang, N., Duchenne, O., Çelebi, O., Alrassy, P., Zhang, P., Li, P., Vasic, P., Weng, P., Bhargava, P., Dubal, P., Krishnan, P., Koura, P. S., Xu, P., He, Q., Dong, Q., Srinivasan, R., Ganapathy, R., Calderer, R., Cabral, R. S., Stojnic, R., Raileanu, R., Maheswari, R., Girdhar, R., Patel, R., Sauvestre, R., Polidoro, R., Sumbaly, R., Taylor, R., Silva, R., Hou, R., Wang, R., Hosseini, S., Chennabasappa, S., Singh, S., Bell, S., Kim, S. S., Edunov, S., Nie, S., Narang, S., Raparthy, S., Shen, S., Wan, S., Bhosale, S., Zhang, S., Vandenhende, S., Batra, S., Whitman, S., Sootla, S., Collot, S., Gururangan, S., Borodinsky, S., Herman, T., Fowler, T., Sheasha, T., Georgiou, T., Scialom, T., Speckbacher, T., Mihaylov, T., Xiao, T., Karn, U., Goswami, V., Gupta, V., Ramanathan, V., Kerkez, V., Gonguet, V., Do, V., Vogeti, V., Albiero, V., Petrovic, V., Chu, W., Xiong, W., Fu, W., Meers, W., Martinet, X., Wang, X., Wang, X., Tan, X. E., Xia, X., Xie, X., Jia, X., Wang, X., Goldschlag, Y., Gaur, Y., Babaei, Y., Wen, Y., Song, Y., Zhang, Y., Li, Y., Mao, Y., Coudert, Z. D., Yan, Z., Chen, Z., Papakipos, Z., Singh, A., Srivastava, A., Jain, A., Kelsey, A., Shajnfeld, A., Gangidi, A., Victoria, A., Goldstand, A., Menon, A., Sharma, A., Boesenberg, A., Baevski, A., Feinstein, A., Kallet, A., Sangani, A., Teo, A., Yunus, A., Lupu, A., Alvarado, A., Caples, A., Gu, A., Ho, A., Poulton, A., Ryan, A., Ramchandani, A., Dong, A., Franco, A., Goyal, A., Saraf, A., Chowdhury, A., Gabriel, A., Bharambe, A., Eisenman, A., Yazdan, A., James, B., Maurer, B., Leonhardi, B., Huang, B., Loyd, B., Paola, B. D., Paranjape, B., Liu, B., Wu, B., Ni, B., Hancock, B., Wasti, B., Spence, B., Stojkovic, B., Gamido, B., Montalvo, B., Parker, C., Burton, C., Mejia, C., Liu, C., Wang, C., Kim, C., Zhou, C., Hu, C., Chu, C.-H., Cai, C., Tindal, C., Feichtenhofer, C., Gao, C., Civin, D., Beaty, D., Kreymer, D., Li, D., Adkins, D., Xu, D., Testuggine, D., David, D., Parikh, D., Liskovich, D., Foss, D., Wang, D., Le, D., Holland, D., Dowling, E., Jamil, E., Montgomery, E., Presani, E., Hahn, E., Wood, E., Le, E.-T., Brinkman, E., Arcaute, E., Dunbar, E., Smothers, E., Sun, F., Kreuk, F., Tian, F., Kokkinos, F., Ozgenel, F., Caggioni, F., Kanayet, F., Seide, F., Florez, G. M., Schwarz, G., Badeer, G., Swee, G., Halpern, G., Herman, G., Sizov, G., Guangyi, Zhang, Lakshminarayanan, G., Inan, H., Shojanazeri, H., Zou, H., Wang, H., Zha, H., Habeeb, H., Rudolph, H., Suk, H., Asperegn, H., Goldman, H., Zhan, H., Damlaj, I., Molybog, I., Tufanov, I., Leontiadis, I., Veliche, I.-E., Gat, I., Weissman, J., Geboski, J., Kohli, J., Lam, J., Asher, J., Gaya, J.-B., Marcus, J., Tang, J., Chan, J., Zhen, J., Reizenstein, J., Teboul, J., Zhong, J., Jin, J., Yang, J., Cummings, J., Carvill, J., Shepard, J., McPhie, J., Torres, J., Ginsburg, J., Wang, J., Wu, K., U, K. H., Saxena, K., Khandelwal, K., Zand, K., Matosich, K., Veeraraghavan, K., Michelena, K., Li, K., Jagadeesh, K., Huang, K., Chawla, K., Huang, K., Chen, L., Garg, L., A. L., Silva, L., Bell, L., Zhang, L., Guo, L., Yu, L., Moshkovich, L., Wehrstedt, L., Khassa, M., Avalani, M., Bhatt, M., Mankus, M., Hasson, M., Lennie, M., Reso, M., Groshev, M., Naumov, M., Lathi, M., Keneally, M., Liu, M., Seltzer, M. L., Valko, M., Restrepo, M., Patel, M., Vyatskov, M., Samvelyan, M., Clark, M., Macey, M., Wang, M., Hermoso, M. J., Metanat, M., Rastegari, M., Bansal, M., Santhanam, N., Parks, N., White, N., Bawa, N., Singhal, N., Egebo, N., Usunier, N., Mehta, N., Laptev, N. P., Dong, N., Cheng, N., Chernoguz, O., Hart, O., Salpekar, O., Kalinli, O., Kent, P., Parekh, P., Saab, P., Balaji, P., Rittner, P., Bontrager, P., Roux, P., Dollar, P., Zvyagina, P., Ratanchandani, P., Yuvraj, P., Liang, Q., Alao, R., Rodriguez, R., Ayub, R., Murthy, R., Nayani, R., Mitra, R., Parthasarathy, R., Li, R., Hogan, R., Battey, R., Wang, R., Howes, R., Rinott, R., Mehta, S., Siby, S., Bondu, S. J., Datta, S., Chugh, S., Hunt, S., Dhillon, S., Sidorov, S., Pan, S., Mahajan, S., Verma, S., Yamamoto, S., Ramaswamy, S., Lindsay, S., Lindsay, S., Feng, S., Lin, S., Zha, S. C., Patil, S., Shankar, S., Zhang, S., Zhang, S., Wang, S., Agarwal, S., Sajuyigbe, S., Chintala, S., Max, S., Chen, S., Kehoe, S., Satterfield, S., Govindaprasad, S., Gupta, S., Deng, S., Cho, S., Virk, S., Subramanian, S., Choudhury, S., Goldman, S., Remez, T., Glaser, T., Best, T., Koehler, T., Robinson, T., Li, T., Zhang, T., Matthews, T., Chou, T., Shaked, T., Vontimitta, V., Ajayi, V., Montanez, V., Mohan, V., Kumar, V. S., Mangla, V., Ionescu, V., Poenaru, V., Mihailescu, V. T., Ivanov, V., Li, W., Wang, W., Jiang, W., Bouaziz, W., Constable, W., Tang, X., Wu, X., Wang, X., Wu, X., Gao, X., Kleinman, Y., Chen, Y., Hu, Y., Jia, Y., Qi, Y., Li, Y., Zhang, Y., Zhang, Y., Adi, Y., Nam, Y., Yu, Wang, Zhao, Y., Hao, Y., Qian, Y., Li, Y., He, Y., Rait, Z., DeVito, Z., Rosnbrick, Z., Wen, Z., Yang, Z., Zhao, Z., and Ma, Z. The llama 3 herd of models, 2024. URL <https://arxiv.org/abs/2407.21783>.

Hendrycks, D., Burns, C., Kadavath, S., Arora, A., Basart, S., Tang, E., Song, D., and Steinhardt, J. Measuring mathematical problem solving with the MATH dataset. In *Thirty-fifth Conference on Neural Information Processing Systems Datasets and Benchmarks Track (Round 2)*, 2021. URL <https://openreview.net/forum?id=7Bywt2mQsCe>.

Huang, Y., Cheng, Y., and Liang, Y. In-context convergence of transformers. In Salakhutdinov, R., Kolter, Z., Heller, K., Weller, A., Oliver, N., Scarlett, J., and Berkenkamp, F. (eds.), *Proceedings of the 41st International Conference on Machine Learning*, volume 235 of *Proceedings of Machine Learning Research*, pp. 19660–19722. PMLR, 21–27 Jul 2024. URL <https://proceedings.mlr.press/v235/huang24d.html>.

Joren, H., Zhang, J., Ferng, C.-S., Juan, D.-C., Taly, A., and Rashtchian, C. Sufficient context: A new lens on retrieval augmented generation systems. In *The Thirteenth International Conference on Learning Representations*, 2025. URL <https://openreview.net/forum?id=Jjr20dj8DJ>.

Kapuriya, J., Kaushik, M., Ganguly, D., and Bhatia, S. Exploring the role of diversity in example selection for in-context learning. In *Proceedings of the 48th International ACM SIGIR Conference on Research and Development in Information Retrieval*, SIGIR ’25, pp. 2962–2966, New York, NY, USA, 2025. Association for Computing Machinery. ISBN 9798400715921. doi: 10.1145/3726302.3730194. URL <https://doi.org/10.1145/3726302.3730194>.

Karpukhin, V., Oguz, B., Min, S., Lewis, P., Wu, L., Edunov, S., Chen, D., and Yih, W.-t. Dense passage retrieval for open-domain question answering. In Weber, B., Cohn, T., He, Y., and Liu, Y. (eds.), *Proceedings of the 2020 Conference on Empirical Methods in Natural Language Processing (EMNLP)*, pp. 6769–6781, Online, November 2020. Association for Computational Linguistics. doi: 10.18653/v1/2020.emnlp-main.550. URL <https://aclanthology.org/2020.emnlp-main.550/>.

Kweon, W., Kang, S., Tian, R., Jiang, P., Han, J., and Yu, H. Topic coverage-based demonstration retrieval for in-context learning. In Christodoulopoulos, C., Chakraborty, T., Rose, C., and Peng, V. (eds.), *Proceedings of the 2025 Conference on Empirical Methods in Natural Language Processing*, pp. 19911–19923, Suzhou, China, November 2025. Association for Computational Linguistics. ISBN 979-8-89176-332-6. doi: 10.18653/v1/2025.emnlp-main.1007. URL <https://aclanthology.org/2025.emnlp-main.1007/>.

Kwiatkowski, T., Palomaki, J., Redfield, O., Collins, M., Parikh, A., Alberti, C., Epstein, D., Polosukhin, I., Devlin, J., Lee, K., Toutanova, K., Jones, L., Kelcey, M., Chang, M.-W., Dai, A. M., Uszkoreit, J., Le, Q., and Petrov, S. Natural questions: A benchmark for question answering research. *Transactions of the Association for Computational Linguistics*, 7:452–466, 2019. doi: 10.1162/tacl\_a\_00276. URL <https://aclanthology.org/Q19-1026/>.

Kwon, W., Li, Z., Zhuang, S., Sheng, Y., Zheng, L., Yu, C. H., Gonzalez, J. E., Zhang, H., and Stoica, I. Efficient memory management for large language model serving with pagedattention. In *Proceedings of the ACM SIGOPS 29th Symposium on Operating Systems Principles*, 2023.

Li, H., Wang, M., Lu, S., Cui, X., and Chen, P.-Y. How do nonlinear transformers learn and generalize in in-context learning? In *Forty-first International Conference on Machine Learning*, 2024. URL <https://openreview.net/forum?id=I4HTPws9P6>.

Li, Y., Zhang, W., Yang, Y., Huang, W.-C., Wu, Y., Luo, J., Bei, Y., Zou, H. P., Luo, X., Zhao, Y., Chan, C., Chen, Y., Deng, Z., Li, Y., Zheng, H.-T., Li, D., Jiang, R., Zhang, M., Song, Y., and Yu, P. S. A survey of RAG-reasoning systems in large language models. In Christodoulopoulos, C., Chakraborty, T., Rose, C., and Peng, V. (eds.), *Findings of the Association for Computational Linguistics: EMNLP 2025*, pp. 12120–12145, Suzhou, China, November 2025. Association for Computational Linguistics. ISBN 979-8-89176-335-7. doi: 10.18653/v1/2025.findings-emnlp.648. URL <https://aclanthology.org/2025.findings-emnlp.648/>.

Lightman, H., Kosaraju, V., Burda, Y., Edwards, H., Baker, B., Lee, T., Leike, J., Schulman, J., Sutskever, I., and Cobbe, K. Let’s verify step by step. In *The Twelfth International Conference on Learning Representations*, 2024. URL <https://openreview.net/forum?id=v8L0pN6EOi>.

Liu, Z., Zhang, R., Wang, Z., Yan, M., Yang, Z., Hovland, P. D., Nicolae, B., Cappello, F., Tang, S., and Zhang, Z. CoLA: Compute-efficient pre-training of LLMs via low-rank activation. In Christodoulopoulos, C., Chakraborty, T., Rose, C., and Peng, V. (eds.), *Proceedings of the 2025 Conference on Empirical Methods in Natural Language Processing*, pp. 4627–4645, Suzhou, China, November 2025. Association for Computational Linguistics. ISBN 979-8-89176-332-6. doi: 10.18653/v1/2025.emnlp-main.230. URL <https://aclanthology.org/2025.emnlp-main.230/>.

Lu, Y. M., Letey, M., Zavatone-Veth, J. A., Maiti, A., and Pehlevan, C. Asymptotic theory of in-context learning by

linear attention. *Proceedings of the National Academy of Sciences*, 122(28), July 2025. ISSN 1091-6490. doi: 10.1073/pnas.2502599122. URL <http://dx.doi.org/10.1073/pnas.2502599122>.

Luo, J., Tian, Y., Cao, C., Luo, Z., Lin, H., Li, K., Kong, C., Yang, R., and Ma, J. From storage to experience: A survey on the evolution of llm agent memory mechanisms. *Preprints*, January 2026. doi: 10.20944/preprints202601.0618.v2. URL <https://doi.org/10.20944/preprints202601.0618.v2>.

Mahankali, A. V., Hashimoto, T., and Ma, T. One step of gradient descent is provably the optimal in-context learner with one layer of linear self-attention. In *The Twelfth International Conference on Learning Representations*, 2024. URL <https://openreview.net/forum?id=8p3fu561Kc>.

Mao, Y., Kim, Y., and Zhou, Y. CHAMP: A competition-level dataset for fine-grained analyses of LLMs' mathematical reasoning capabilities. In Ku, L.-W., Martins, A., and Srikumar, V. (eds.), *Findings of the Association for Computational Linguistics: ACL 2024*, pp. 13256–13274, Bangkok, Thailand, August 2024. Association for Computational Linguistics. doi: 10.18653/v1/2024.findings-acl.785. URL <https://aclanthology.org/2024.findings-acl.785>.

Mei, L., Yao, J., Ge, Y., Wang, Y., Bi, B., Cai, Y., Liu, J., Li, M., Li, Z.-Z., Zhang, D., Zhou, C., Mao, J., Xia, T., Guo, J., and Liu, S. A survey of context engineering for large language models, 2025. URL <https://arxiv.org/abs/2507.13334>.

Mistral AI team. Un ministral, des ministraux. <https://mistral.ai/news/ministraux>, oct 2024. Accessed: 2025-11-18.

Nguyen, A. and Reddy, G. Differential learning kinetics govern the transition from memorization to generalization during in-context learning. In *The Thirteenth International Conference on Learning Representations*, 2025. URL <https://openreview.net/forum?id=INyi7qUdjZ>.

Park, C. F., Lubana, E. S., and Tanaka, H. Competition dynamics shape algorithmic phases of in-context learning. In *The Thirteenth International Conference on Learning Representations*, 2025. URL <https://openreview.net/forum?id=XgH1wfHSX8>.

Rein, D., Hou, B. L., Stickland, A. C., Petty, J., Pang, R. Y., Dirani, J., Michael, J., and Bowman, S. R. GPQA: A graduate-level google-proof q&a benchmark. In *First Conference on Language Modeling*, 2024. URL <https://openreview.net/forum?id=Ti67584b98>.

Smart, M., Bietti, A., and Sengupta, A. M. In-context denoising with one-layer transformers: Connections between attention and associative memory retrieval. In *Forty-second International Conference on Machine Learning*, 2025. URL <https://openreview.net/forum?id=F081zoBgad>.

Suzgun, M., Yuksekgonul, M., Bianchi, F., Jurafsky, D., and Zou, J. Dynamic cheatsheet: Test-time learning with adaptive memory, 2025. URL <https://arxiv.org/abs/2504.07952>.

Vaswani, A., Shazeer, N., Parmar, N., Uszkoreit, J., Jones, L., Gomez, A. N., Kaiser, L. u., and Polosukhin, I. Attention is all you need. In Guyon, I., Luxburg, U. V., Bengio, S., Wallach, H., Fergus, R., Vishwanathan, S., and Garnett, R. (eds.), *Advances in Neural Information Processing Systems*, volume 30. Curran Associates, Inc., 2017. URL [https://proceedings.neurips.cc/paper\\_files/paper/2017/file/3f5ee243547dee91fb053c1c4a845aa-Paper.pdf](https://proceedings.neurips.cc/paper_files/paper/2017/file/3f5ee243547dee91fb053c1c4a845aa-Paper.pdf).

Wei, T., Sachdeva, N., Coleman, B., He, Z., Bei, Y., Ning, X., Ai, M., Li, Y., He, J., Chi, E. H., Wang, C., Chen, S., Pereira, F., Kang, W.-C., and Cheng, D. Z. Evo-memory: Benchmarking llm agent test-time learning with self-evolving memory, 2025a. URL <https://arxiv.org/abs/2511.20857>.

Wei, Z., Chen, W.-L., and Meng, Y. InstructRAG: Instructing retrieval-augmented generation via self-synthesized rationales. In *The Thirteenth International Conference on Learning Representations*, 2025b. URL <https://openreview.net/forum?id=P1qhkp8gQT>.

Wolf, T., Debut, L., Sanh, V., Chaumond, J., Delangue, C., Moi, A., Cistac, P., Rault, T., Louf, R., Funtowicz, M., Davison, J., Shleifer, S., von Platen, P., Ma, C., Jernite, Y., Plu, J., Xu, C., Le Scao, T., Gugger, S., Drame, M., Lhoest, Q., and Rush, A. Transformers: State-of-the-art natural language processing. In Liu, Q. and Schlangen, D. (eds.), *Proceedings of the 2020 Conference on Empirical Methods in Natural Language Processing: System Demonstrations*, pp. 38–45, Online, October 2020. Association for Computational Linguistics. doi: 10.18653/v1/2020.emnlp-demos.6. URL <https://aclanthology.org/2020.emnlp-demos.6>.

Xie, S. M., Pham, H., Dong, X., Du, N., Liu, H., Lu, Y., Liang, P., Le, Q. V., Ma, T., and Yu, A. W. Doremi: optimizing data mixtures speeds up language model pretraining. In *Proceedings of the 37th International Conference on Neural Information Processing Systems*, NIPS '23, Red Hook, NY, USA, 2023. Curran Associates Inc.

Xu, S., Pang, L., Shen, H., and Cheng, X. A theory for token-level harmonization in retrieval-augmented generation. In *The Thirteenth International Conference on Learning Representations*, 2025a. URL <https://openreview.net/forum?id=tbx3u2oZAu>.

Xu, W., Liang, Z., Mei, K., Gao, H., Tan, J., and Zhang, Y. A-mem: Agentic memory for llm agents, 2025b. URL <https://arxiv.org/abs/2502.12110>.

Yang, A., Li, A., Yang, B., Zhang, B., Hui, B., Zheng, B., Yu, B., Gao, C., Huang, C., Lv, C., Zheng, C., Liu, D., Zhou, F., Huang, F., Hu, F., Ge, H., Wei, H., Lin, H., Tang, J., Yang, J., Tu, J., Zhang, J., Yang, J., Yang, J., Zhou, J., Zhou, J., Lin, J., Dang, K., Bao, K., Yang, K., Yu, L., Deng, L., Li, M., Xue, M., Li, M., Zhang, P., Wang, P., Zhu, Q., Men, R., Gao, R., Liu, S., Luo, S., Li, T., Tang, T., Yin, W., Ren, X., Wang, X., Zhang, X., Ren, X., Fan, Y., Su, Y., Zhang, Y., Zhang, Y., Wan, Y., Liu, Y., Wang, Z., Cui, Z., Zhang, Z., Zhou, Z., and Qiu, Z. Qwen3 technical report, 2025. URL <https://arxiv.org/abs/2505.09388>.

Yang, T., Huang, Y., Liang, Y., and Chi, Y. In-context learning with representations: Contextual generalization of trained transformers. In *The Thirty-eighth Annual Conference on Neural Information Processing Systems*, 2024. URL <https://openreview.net/forum?id=ik37kKxKBm>.

Yun, T., Oh, J., Min, H., Lee, Y., Bang, J., Cai, J., and Song, H. Refeed: Multi-dimensional summarization refinement with reflective reasoning on feedback. In *Second Conference on Language Modeling*, 2025. URL <https://openreview.net/forum?id=6BGDGKZN7q>.

Zhang, R., Frei, S., and Bartlett, P. L. Trained transformers learn linear models in-context. *J. Mach. Learn. Res.*, 25(1), January 2024. ISSN 1532-4435.

Zhang, Z., Lan, S., Song, L., Bian, J., Li, Y., and Ren, K. Learning to select in-context demonstration preferred by large language model. In Che, W., Nabende, J., Shutova, E., and Pilehvar, M. T. (eds.), *Findings of the Association for Computational Linguistics: ACL 2025*, pp. 11345–11360, Vienna, Austria, July 2025. Association for Computational Linguistics. ISBN 979-8-89176-256-5. doi: 10.18653/v1/2025.findings-acl.592. URL [https://aclanthology.org/2025.findings-acl.592/](https://aclanthology.org/2025.findings-acl.592).

Zhao, A., Huang, D., Xu, Q., Lin, M., Liu, Y.-J., and Huang, G. Expel: Llm agents are experiential learners. In *Proceedings of the Thirty-Eighth AAAI Conference on Artificial Intelligence and Thirty-Sixth Conference on Innovative Applications of Artificial Intelligence and Fourteenth Symposium on Educational Advances in Artificial Intelligence*, AAAI'24/IAAI'24/EAAI'24. AAAI Press, 2024. ISBN 978-1-57735-887-9. doi: 10.1609/aaai.v38i17.29936. URL <https://doi.org/10.1609/aaai.v38i17.29936>.

Zhou, Y., Li, J., Xiang, Y., Yan, H., Gui, L., and He, Y. The mystery of in-context learning: A comprehensive survey on interpretation and analysis. In Al-Onaizan, Y., Bansal, M., and Chen, Y.-N. (eds.), *Proceedings of the 2024 Conference on Empirical Methods in Natural Language Processing*, pp. 14365–14378, Miami, Florida, USA, November 2024. Association for Computational Linguistics. doi: 10.18653/v1/2024.emnlp-main.795. URL [https://aclanthology.org/2024.emnlp-main.795/](https://aclanthology.org/2024.emnlp-main.795).

## A. Proof

### A.1. Supporting Lemma

We first present two lemmas about the Lipschitz constants of the attention mechanism and the MLP.

#### Lemma 6.

$$\delta_{\text{attn}}(t, x) = \alpha_{x \leftarrow t} W_O (v_t - v_x) = \alpha_{x \leftarrow t} W_O \Delta v.$$

*Proof of Lemma 6.* The attention contribution at position  $x$  is

$$\text{AttnOut}_x([t, x]) = W_O (\alpha_{x \leftarrow t} v_t + \alpha_{x \leftarrow x} v_x).$$

In the case without context knowledge, the row-wise softmax has a single weight equal to 1, so

$$\text{AttnOut}_x([x]) = W_O v_x.$$

The attention layer includes a residual connection  $+x$ , which is the same under both inputs. Hence the difference between the two outputs comes entirely from the attention term, which is

$$\begin{aligned} \text{AttnOut}_x([t, x]) - \text{AttnOut}_x([x]) \\ = W_O (\alpha_{x \leftarrow t} v_t + \alpha_{x \leftarrow x} v_x - v_x) \\ = \alpha_{x \leftarrow t} W_O (v_t - v_x). \end{aligned}$$

□

**Lemma 7.** For any  $z, z' \in \mathbb{R}^d$ ,

$$\|\text{MLP}(z) - \text{MLP}(z')\| \leq L_{\text{MLP}} \|z - z'\|,$$

$$L_{\text{MLP}} = 1 + \|W_2\| \|W_1\|.$$

*Proof of Lemma 7.* Let  $g(z) := W_2 \sigma(W_1 z)$ . Since  $\sigma$  is 1-Lipschitz, we have

$$\begin{aligned} \|g(z) - g(z')\| &\leq \|W_2\| \|\sigma(W_1 z) - \sigma(W_1 z')\| \\ &\leq \|W_2\| \|W_1\| \|z - z'\|. \end{aligned}$$

Therefore,

$$\begin{aligned} \|\text{MLP}(z) - \text{MLP}(z')\| \\ = \|z - z' + g(z) - g(z')\| \\ \leq \|z - z'\| + \|g(z) - g(z')\| \\ \leq (1 + \|W_2\| \|W_1\|) \|z - z'\|. \end{aligned}$$

□

### A.2. Proof of Theorem 2

*Proof of Theorem 2.* Let  $z_0 = \text{Attn}_x([x])$  and  $z_1 = \text{Attn}_x([t, x])$  denote the outputs of the attention layer when attending only to  $x$  and when attending to both  $t$  and  $x$ , respectively. By Lemma 6, the difference between these two inputs is

$$z_1 - z_0 = \delta_{\text{attn}}(t, x).$$

We construct a linear path between  $z_0$  and  $z_1$ , parameterized as  $z(s) = z_0 + s(z_1 - z_0)$  for  $s \in [0, 1]$ , i.e.,

$$z(s) = \text{Attn}_x([x]) + s \delta_{\text{attn}}(t, x).$$

By the fundamental theorem of calculus, the difference of a vector-valued function along this path equals the integral of its derivative:

$$\begin{aligned} e(t, x) - e(x) &= \text{MLP}(z_1) - \text{MLP}(z_0) \\ &= \int_0^1 \frac{d}{ds} \text{MLP}(z(s)) ds. \end{aligned}$$

Applying the chain rule and using the Jacobian of the MLP,  $J_{\text{MLP}}(z) = \frac{\partial \text{MLP}(z)}{\partial z}$ , we obtain

$$\begin{aligned} \frac{d}{ds} \text{MLP}(z(s)) &= J_{\text{MLP}}(z(s)) \cdot \frac{dz(s)}{ds} \\ &= J_{\text{MLP}}(z(s)) \cdot \delta_{\text{attn}}(t, x). \end{aligned}$$

Substituting this into the integral formula gives

$$\begin{aligned} e(t, x) - e(x) &= \\ &\int_0^1 J_{\text{MLP}}(\text{Attn}_x([x]) + s \delta_{\text{attn}}(t, x)) \delta_{\text{attn}}(t, x) ds. \end{aligned}$$

Comparing with the definition of  $g(t, x)$  in Definition 1, we see that the right-hand side is exactly  $g(t, x)$ . Hence

$$e(t, x) = e(x) + g(t, x).$$

□

### A.3. Proof of Theorem 3

*Proof of Theorem 3.* Recall the contextual vector (Definition 1)

$$g(t, x) = \int_0^1 J_{\text{MLP}}(\text{Attn}_x([x]) + s \delta_{\text{attn}}(t, x)) \delta_{\text{attn}}(t, x) ds.$$

Vector Norm. Using the submultiplicativity of the operator norm and the triangle inequality,

$$\begin{aligned} \|g(t, x)\| &\leq \\ &\int_0^1 \|J_{\text{MLP}}(\text{Attn}_x([x]) + s \delta_{\text{attn}}(t, x))\| \|s \delta_{\text{attn}}(t, x)\| ds. \end{aligned}$$

By the Jacobian form of the MLP,

$$J_{\text{MLP}}(z) := I + W_2 J_\sigma(W_1 z) W_1, \quad \|J_\sigma(\cdot)\| \leq 1 \text{ a.e.},$$

we have, for almost every  $z$ ,

$$\begin{aligned} \|J_{\text{MLP}}(z)\| &\leq \|I\| + \|W_2\| \|J_\sigma(W_1 z)\| \|W_1\| \\ &\leq 1 + \|W_2\| \|W_1\| \\ &= L_{\text{MLP}}. \end{aligned}$$

Therefore,

$$\begin{aligned} \|g(t, x)\| &\leq \int_0^1 L_{\text{MLP}} \|\delta_{\text{attn}}(t, x)\| \, ds \\ &= L_{\text{MLP}} \|\delta_{\text{attn}}(t, x)\|. \end{aligned}$$

Finally, by Lemma 6,  $\delta_{\text{attn}}(t, x) = \alpha_{x \leftarrow t} W_O (v_t - v_x)$ , hence

$$\|\delta_{\text{attn}}(t, x)\| \leq \alpha_{x \leftarrow t} \|W_O\| \|v_t - v_x\|,$$

which yields

$$\begin{aligned} \|g(t, x)\| &\leq L_{\text{MLP}} \|\delta_{\text{attn}}(t, x)\| \\ &\leq L_{\text{MLP}} \alpha_{x \leftarrow t} \|W_O\| \|v_t - v_x\|. \end{aligned}$$

Vector Direction. By Theorem 2,  $e(t, x) = e(x) + g(t, x)$ . If  $\|e(t, x)\| < \|e(x)\|$ , then

$$\|e(x) + g(t, x)\|^2 < \|e(x)\|^2.$$

Expanding the left-hand side gives

$$\|e(x)\|^2 + 2\langle e(x), g(t, x) \rangle + \|g(t, x)\|^2 < \|e(x)\|^2,$$

so

$$\begin{aligned} 2\langle e(x), g(t, x) \rangle + \|g(t, x)\|^2 &< 0 \iff \\ \langle -e(x), g(t, x) \rangle &> \frac{\|g(t, x)\|^2}{2}. \end{aligned}$$

Dividing both sides by  $\|e(x)\| \|g(t, x)\|$  yields

$$\frac{\langle -e(x), g(t, x) \rangle}{\|e(x)\| \|g(t, x)\|} > \frac{\|g(t, x)\|}{2\|e(x)\|}.$$

Recalling the definition of

$$\rho(t, x) := \frac{\langle -e(x), g(t, x) \rangle}{\|e(x)\| \|g(t, x)\|} \in [-1, 1],$$

we obtain the desired necessary condition

$$\rho(t, x) > \frac{\|g(t, x)\|}{2\|e(x)\|}.$$

#### A.4. Proof of Corollary 4

*Proof of Corollary 4.* Let  $\alpha_{x \leftarrow t_{n+1}} := A_{x t_{n+1}}$ . Analogously to Lemma 6, the increment in the attention output at position  $x$  is

$$\begin{aligned} \delta_{\text{attn}}(t_{n+1} | T, x) &:= \text{AttnOut}_x([T \cup \{t_{n+1}\}, x]) - \text{AttnOut}_x([T, x]) \\ &= W_O \alpha_{x \leftarrow t_{n+1}} (v_{t_{n+1}} - \bar{v}_T). \end{aligned}$$

Following Definition 1, we define the incremental information vector contributed by the new token as

$$\begin{aligned} g(t_{n+1} | T, x) &:= \\ &\int_0^1 J_{\text{MLP}}(\text{Attn}_x([T, x]) + s \delta_{\text{attn}}(t_{n+1} | T, x)) \\ &\quad \delta_{\text{attn}}(t_{n+1} | T, x) \, ds. \end{aligned}$$

Then we have  $e(T \cup \{t_{n+1}\}, x) = e(T, x) + g(t_{n+1} | T, x)$ . By following the same proof strategy as in Theorem 2 and Theorem 3, we obtain the corresponding statements in Theorem 3.  $\square$

#### A.5. Proof of Corollary 5

*Proof of Corollary 5.* We prove the stated norm bound and direction condition for the overall vector

$$g^{(L)}(t, x) := \sum_{\ell=1}^L \tilde{g}^{(\ell)}(t, x),$$

$$e^{(L)}(t, x) = e^{(L)}(x) + g^{(L)}(t, x).$$

Vector Norm. Fix a layer  $\ell$ . By definition,

$$\begin{aligned} g^{(\ell)}(t, x) &= \\ &\int_0^1 J_{\text{MLP}^{(\ell)}}(\text{Attn}_x^{(\ell)}([x]) + s \delta_{\text{attn}}^{(\ell)}(t, x)) \delta_{\text{attn}}^{(\ell)}(t, x) \, ds. \end{aligned}$$

As in the single-layer case, using  $\|J_{\text{MLP}^{(\ell)}}(\cdot)\| \leq L_{\text{MLP}}^{(\ell)}$  (a.e.) gives

$$\|g^{(\ell)}(t, x)\| \leq L_{\text{MLP}}^{(\ell)} \|\delta_{\text{attn}}^{(\ell)}(t, x)\|.$$

Moreover, from

$$\begin{aligned} \delta_{\text{attn}}^{(\ell)}(t, x) &= \alpha_{x \leftarrow t}^{(\ell)} W_O^{(\ell)} \Delta v^{(\ell)}, \\ \Delta v^{(\ell)} &:= v_t^{(\ell)} - v_x^{(\ell)}, \end{aligned}$$

we have

$$\|\delta_{\text{attn}}^{(\ell)}(t, x)\| \leq \alpha_{x \leftarrow t}^{(\ell)} \|W_O^{(\ell)}\| \|v_t^{(\ell)} - v_x^{(\ell)}\|.$$

Hence

$$\square \quad \|g^{(\ell)}(t, x)\| \leq L_{\text{MLP}}^{(\ell)} \alpha_{x \leftarrow t}^{(\ell)} \|W_O^{(\ell)}\| \|v_t^{(\ell)} - v_x^{(\ell)}\|.$$

Next, consider the propagation through the upper layers. Recall

$$\tilde{g}^{(\ell)}(t, x) = \int_0^1 J_{\Phi^{(\ell+1:L)}}(h_x^{(\ell)}(x) + s g^{(\ell)}(t, x)) g^{(\ell)}(t, x) ds,$$

where  $\Phi^{(\ell+1:L)} = B_x^{(L)} \circ \dots \circ B_x^{(\ell+1)}$ . If each residual block  $B_x^{(j)}$  is  $L_{\text{blk}}^{(j)}$ -Lipschitz, then the composition  $\Phi^{(\ell+1:L)}$  is

$$\left( \prod_{j=\ell+1}^L L_{\text{blk}}^{(j)} \right) \text{-Lipschitz.}$$

Consequently, the Jacobian norm is bounded almost everywhere by the same constant, i.e.,

$$\|J_{\Phi^{(\ell+1:L)}}(z)\| \leq \prod_{j=\ell+1}^L L_{\text{blk}}^{(j)} \quad \text{for a.e. } z.$$

Therefore,

$$\begin{aligned} \|\tilde{g}^{(\ell)}(t, x)\| &\leq \int_0^1 \left( \prod_{j=\ell+1}^L L_{\text{blk}}^{(j)} \right) \|g^{(\ell)}(t, x)\| ds \\ &= \left( \prod_{j=\ell+1}^L L_{\text{blk}}^{(j)} \right) \|g^{(\ell)}(t, x)\|. \end{aligned}$$

Combining the above bounds and summing over  $\ell$  yields

$$\begin{aligned} &\|g^{(L)}(t, x)\| \\ &= \left\| \sum_{\ell=1}^L \tilde{g}^{(\ell)}(t, x) \right\| \leq \sum_{\ell=1}^L \|\tilde{g}^{(\ell)}(t, x)\| \\ &\leq \sum_{\ell=1}^L \left( \prod_{j=\ell+1}^L L_{\text{blk}}^{(j)} \right) L_{\text{MLP}}^{(\ell)} \alpha_{x \leftarrow t}^{(\ell)} \|W_O^{(\ell)}\| \|v_t^{(\ell)} - v_x^{(\ell)}\|, \end{aligned}$$

which is exactly the stated bound.

*Vector Direction.* Using the error decomposition  $e^{(L)}(t, x) = e^{(L)}(x) + g^{(L)}(t, x)$ , similar with the proof of Theorem 3, we can derive that

$$\langle -e^{(L)}(x), g^{(L)}(t, x) \rangle > \frac{\|g^{(L)}(t, x)\|^2}{2}.$$

If  $\|g^{(L)}(t, x)\| > 0$ , dividing both sides by  $\|e^{(L)}(x)\| \|g^{(L)}(t, x)\|$  yields

$$\rho^{(L)}(t, x) := \frac{\langle -e^{(L)}(x), g^{(L)}(t, x) \rangle}{\|e^{(L)}(x)\| \|g^{(L)}(t, x)\|} > \frac{\|g^{(L)}(t, x)\|}{2 \|e^{(L)}(x)\|},$$

which proves the stated condition.  $\square$

## B. Additional Information

### B.1. Experimental Datasets

**MATH** MATH is a competition-style mathematics benchmark designed to measure advanced symbolic and multi-step problem solving. It contains 12.5k problems drawn from high-school math contests and textbooks, spanning multiple subjects (e.g., algebra, geometry, number theory, counting & probability, etc.) and difficulty levels. Each example provides a problem statement together with a full, human-written step-by-step solution and a final boxed answer, which supports evaluating both final-answer correctness and intermediate reasoning. In LLM evaluation, MATH is typically scored by exact match on the final answer (often after normalization). We employ the MATH500 (Lightman et al., 2024) version for our experiments.

**CHAMP** CHAMP (Concept and Hint-Annotated Math Problems) is a competition-level math dataset built for fine-grained analysis of how models use contextual information. Beyond the original problem and gold solution/answer, each instance is annotated with (1) concepts—general mathematical facts or principles that may be relevant—and (2) hints—problem-specific tricks or guidance that can materially help solve the problem. This structure enables controlled experiments such as adding helpful hints, injecting misleading concepts, or testing whether models can benefit from the “right” side information. CHAMP is also used to study solution faithfulness and verification, not just final-answer accuracy.

**TheoremQA** TheoremQA is a theorem-driven question answering benchmark that tests whether models can apply domain knowledge (i.e., specific theorems) to solve challenging problems. It consists of expert-curated questions covering hundreds of theorems across multiple disciplines, including mathematics, physics, EE/CS, and finance. Problems are designed so that solving them requires identifying and correctly using an appropriate theorem rather than relying on surface patterns. The dataset emphasizes reasoning and knowledge application: models must connect the question to relevant formal principles and carry out multi-step derivations to reach the final answer. Evaluation commonly focuses on final-answer accuracy (often exact match), with optional analysis of reasoning quality.

**MMLU-Redux** MMLU-Redux is a cleaned, manually re-annotated variant of the widely used MMLU benchmark, aiming to correct ambiguities and label errors that can distort model comparisons. It preserves the broad subject coverage of MMLU (spanning dozens of academic and professional domains) while providing revised gold answers and improved quality control. The benchmark is intended for more reliable measurement of factual recall and reasoning

in a multiple-choice setting, and it is particularly useful for checking whether model rankings are robust to dataset noise. In practice, evaluation remains standard multiple-choice accuracy, but conclusions are less sensitive to flawed items.

**GPQA** GPQA is a graduate-level, “Google-proof” multiple-choice QA benchmark written by domain experts to be exceptionally difficult even with unrestricted web access. It focuses on deep scientific reasoning in three core areas: biology, chemistry, and physics. The questions are designed to resist shallow retrieval and require substantial conceptual understanding and careful elimination of distractors. Because humans without specialized expertise struggle on the dataset, GPQA is often used to stress-test frontier models and to study oversight and evaluation reliability on hard scientific questions. Performance is typically reported as multiple-choice accuracy, sometimes with analysis by domain and difficulty.

**NaturalQuestions** NaturalQuestions (NQ) is a large-scale QA dataset built from real, anonymized Google search queries paired with Wikipedia pages from top search results. For each question-page pair, human annotators label a long answer (usually a paragraph or section) and a short answer (one or more spans/entities), or mark the question as unanswerable from the page. This design supports both reading comprehension and retrieval-style evaluation, since the system must identify evidence within long documents. NQ includes diverse information-seeking questions and naturally occurring ambiguity, making it a strong benchmark for open-domain QA pipelines. Common metrics include exact match and token-level F1 for short answers, plus long-answer accuracy.

**FinQA** FinQA is a financial question answering dataset targeting numerical reasoning over real corporate reports. Each instance pairs a question with evidence drawn from heterogeneous sources such as tables and accompanying textual context. Solving typically requires multi-step arithmetic, aggregation, and logical operations (e.g., computing growth rates, margins, or differences across periods). A key feature of FinQA is the availability of gold “reasoning programs” (structured operation sequences) that make the computation process explicit, enabling explainable evaluation and program-based training or analysis. Systems are commonly evaluated by final numeric answer accuracy (often exact match after normalization), and sometimes by program correctness or execution validity.

## B.2. Experimental Setup

In this paper, for all three types of contextual information, we use BM25 to retrieve context relevant to the user query.

Table 5. The prompt of inference during our experiments. {information} can be replaced with demonstrations, retrieved knowledge, and memory.

Prompt of Inference
{task_definition}
---
Here are some information to help you solve the given task: ```
{information}
```
---
Based on the above information, solve the following question: {question}

We do not adopt more advanced retrieval methods because our primary goal is to analyze the relationship between the context error and various factors, rather than to optimize performance. To reduce experimental overhead, we employ the relatively simple BM25 method in our analytical experiments.

The inference prompt we used is shown in Table B.2. Specifically, our method designs for different types of information are as follows:

**In-Context Learning** We use a sample ICL approach, where the input consists of the task definition, demonstrations, and the user query, and the output is the answer to the query. The demonstration pool is the training set of each dataset.

**Retrieval-Augmented Generation** We directly use the retrieval corpus provided by each dataset and simply concatenate the retrieved results into the input.

**Memory Evolution** Following Zhao et al. (2024), we implement evolution with a simple agent system consisting of two components: a Thinker and a Reasoner. The Thinker learns from historical interactions and summarizes experience, while the Reasoner answers user queries based on the summarized experience. The Thinker prompt we used is shown in Table 6.

## B.3. Calculation of Main Parameters

In this section, we introduce how to compute each analysis parameter in §4. To reduce the experimental cost, we calculate the following parameters with the first layer of the model, as we consider the first layer as one single Transformer block. **(i)**  $e(x)$  **and**  $e(t, x)$ : We directly compute the

error as the difference between the pooling of the encoding vectors of each output token and the corresponding token in the ground-truth answer, under the inputs  $x$  and  $[t, x]$ , respectively. **(ii)**  $g(t, x)$ : Our computation follows Definition 1, where  $\text{Attn}_x([x])$  and  $\delta_{\text{attn}}(t, x)$  can be obtained directly from the model parameters. For  $J_\sigma$  in  $J_{\text{MLP}}$ , we derive the Jacobian matrices of the activation functions for each LLM accordingly. **(iii)**  $\rho(t, x)$ : Based on the definition in Theorem 3, we can compute it directly from  $e(x)$  and  $g(t, x)$ . **(iv)**  $\alpha_{t \leftarrow x}$ : We directly extract the attention weights from  $x$  to  $t$  when feeding  $[t, x]$  into the model.

## C. Additional Discussion

### C.1. Analysis with Multiple Tokens

Let  $T = (t_1, \dots, t_n)$  be the context sequence and  $X = (x_1, \dots, x_m)$  be the query sequence. We focus on a fixed position  $p$  in  $X$  whose representation is used to form the output. For a single-layer Transformer, denote the attention output at position  $p$  by  $\text{Attn}_p(\cdot)$  and define

$$\delta_{\text{attn}, p}(T, X) := \text{Attn}_p([T, X]) - \text{Attn}_p([X]) \in \mathbb{R}^d.$$

Define the contextual correction vector at position  $p$  as

$$g_p(T, X) :=$$

$$\int_0^1 J_{\text{MLP}}\left(\text{Attn}_p([X]) + s \delta_{\text{attn}, p}(T, X)\right) \delta_{\text{attn}, p}(T, X) ds.$$

By the fundamental theorem of calculus applied to the mapping  $\text{MLP}(\cdot)$  along the line segment  $\text{Attn}_p([X]) \mapsto \text{Attn}_p([T, X])$ , we have

$$y_p([T, X]) - y_p([X]) = g_p(T, X),$$

which implies the same error decomposition as Theorem 2 at position  $p$

$$e_p([T, X]) = e_p([X]) + g_p(T, X).$$

If we define the sequence-level error by concatenation  $e([X]) := [e_1([X]); \dots; e_m([X])] \in \mathbb{R}^{md}$  and similarly  $g(T, X) := [g_1(T, X); \dots; g_m(T, X)]$ , then the decomposition also holds at the sequence level

$$e([T, X]) = e([X]) + g(T, X).$$

Therefore, all geometric implications remain unchanged. In particular, the vector direction defined by the cosine

$$\rho_p(T, X) := \frac{\langle -e_p([X]), g_p(T, X) \rangle}{\|e_p([X])\| \|g_p(T, X)\|} \in [-1, 1]$$

yields the same necessary condition for error reduction

$$\|e_p([T, X])\| < \|e_p([X])\| \Rightarrow \rho_p(T, X) > \frac{\|g_p(T, X)\|}{2\|e_p([X])\|}.$$

### C.2. Effect of Other Structure of Transformer

In this section, we analyze how different factors not discussed in §3 affect the conclusion of this paper.

**Multi-Head Attention.** Multi head attention keeps the same decomposition view because the model still produces an attention output at position  $x$ , and the contextual vector is simply the composition of the per head contributions through the output projection. **Overall, MHA does not change our main conclusion.**

**Attention Variants.** Sharing keys and values across heads mainly redistributes where relevance and complementarity live across heads, while the contextual vector is still governed by how much attention is assigned to the context and how informative the context values are in the projected space. **In short, these variants preserve the key conclusion.**

**Feed Forward Network Variants.** Gating and alternative nonlinearities may alter the local amplification or attenuation of an update, but error reduction still hinges on whether the induced vector aligns with the negative original error and whether its magnitude is not excessively large. **Thus, the main conclusion remains unchanged.**

**Positional Encoding and Attention Bias.** These mechanisms mostly reshape attention weights and therefore affect relevance, yet the same relationship between vector direction, vector norm, and the possibility of error reduction continues to apply. **Consequently, our central conclusion still holds.**

**Masking and Long Context Visibility Constraints.** Visibility constraints decide whether contextual tokens can contribute at all, but whenever they are visible their impact on the error can still be interpreted through the same vector based lens. **So they do not overturn the main conclusion either.**

## C.3. Case Study

We present a case study of our analysis in Table 7.

## D. Additional Experiment

### D.1. Analysis of Multi Information and Multi Layers

In this part, we present how the error change varies with the contextual vector in the multi-context and multi-layer setting, and how the vector varies with the relevance and complementarity of the context, as illustrated in Figures 9 to 12. We can observe that the empirical trends are consistent with the predictions in Corollary 4 and Corollary 5, which

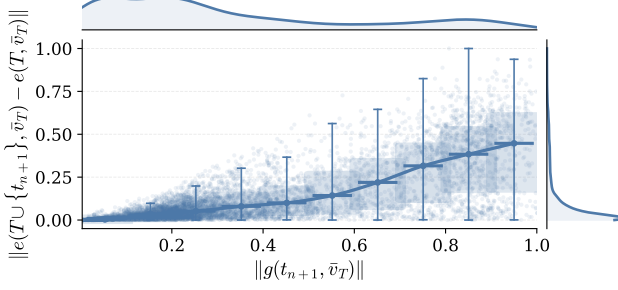


Figure 9. Relationship between error change with new context  $\|e(T \cup \{t_{n+1}\}, x) - e(T, x)\|$  and vector norm  $\|g(t_{n+1} | T, x)\|$ . Each point corresponds to one data sample. The curves at the top and on the right show the marginal distributions of the data points along the  $x$ - and  $y$ -axes, respectively. The fitted Pearson correlation coefficient of the scatter points is 0.751.

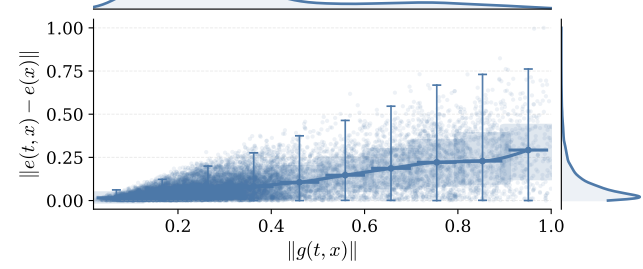


Figure 11. Relationship between multi-layer error change  $\|e^{(L)}(t, x) - e^{(L)}(x)\|$  and the vector norm  $\|g^{(L)}(t, x)\|$ . Each point corresponds to one data sample. The curves at the top and on the right show the marginal distributions of the data points along the  $x$ - and  $y$ -axes, respectively. The fitted Pearson correlation coefficient of the scatter points is 0.655.

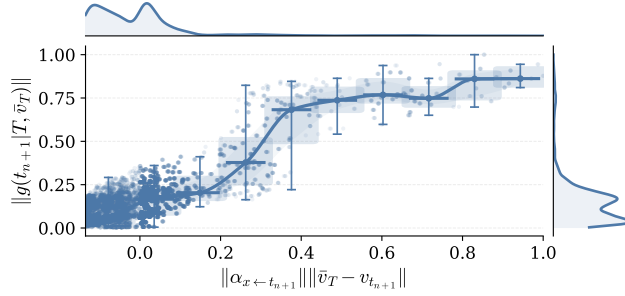


Figure 10. Relationship between the vector norm  $\|g(t_{n+1} | T, x)\|$  and  $\|\alpha_{x \leftarrow t_{n+1}}\| \|\bar{v}_T - v_{t_{n+1}}\|$ . Each point corresponds to one data sample. The curves at the top and on the right show the marginal distributions of the data points along the  $x$ - and  $y$ -axes, respectively. The fitted Pearson correlation coefficient of the scatter points is 0.838.

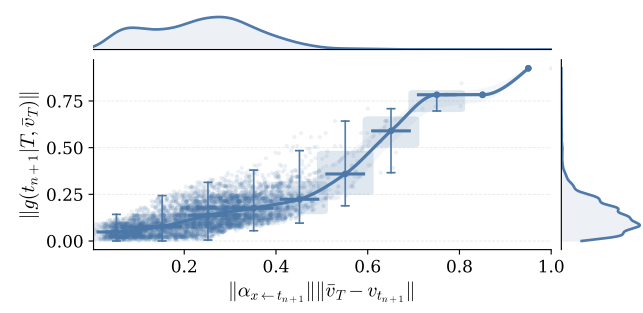


Figure 12. Relationship between the vector norm  $\|g^{(L)}(t, x)\|$  and  $\|\alpha_{x \leftarrow t}^{(L)}\| |t - x|$ . Each point corresponds to one data sample. The curves at the top and on the right show the marginal distributions of the data points along the  $x$ - and  $y$ -axes, respectively. The fitted Pearson correlation coefficient of the scatter points is 0.717.

validate our theoretical derivations.

## D.2. Output Error with Contextual Information cross Different Methods

In this section, we present the analysis of different methods using a single context and a single layer model from Figure 13 to Figure 21.

## D.3. Variation of Contextual Correction Vector with Model Layer

To verify the effect of model depth on the vector as stated in Corollary 5, we compute the context information vector at each layer and plot its variation with respect to the layer index. Because the models have different numbers of layers, we report results on Qwen3-8B and Minstral-8B. Since the first layer mainly reads the input and the last layer mainly produces the final answer, their attention magnitudes are significantly larger than those of intermediate layers, which in turn makes their vectors much larger. To better isolate the effect of depth on the vector, we therefore show the vector from the second to the penultimate layer in Figure 23. For

completeness, Figure 22 also presents the vector across all layers.

From these figures, we observe that: (i) overall, in multi-layer models, the empirical relationships between the context information vector, error change, and the corresponding quantities are consistent with the predictions of Corollary 5, which supports the correctness of our conclusions; and (ii) as the model depth increases, the context information vector tends to increase overall, suggesting that the Lipschitz constants of the layers are collectively smaller than 1, i.e., the model is relatively stable with respect to perturbations.

## D.4. Variation of Contextual Correction Vector with Context Number

To analyze how the number of contexts affects the contextual correction vector, we examine how the contextual correction vector changes under different numbers of contexts. The results are shown in Figure 24, from which we can observe that: (i) Overall, the contextual correction vector does not vary substantially with the number of contexts, which suggests that the model attention to the newly provided con-

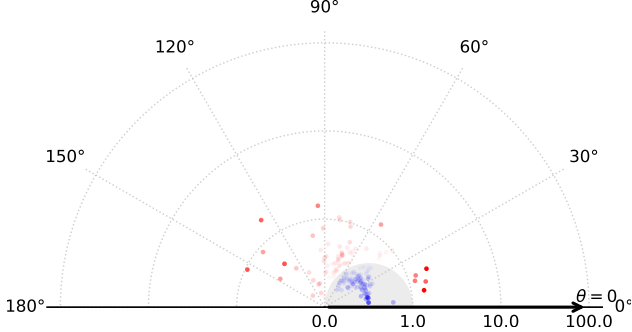


Figure 13. The variation of  $\|e(t, x)\| - \|e(x)\|$  with respect to  $g(t, x)$  of ICL, where each point represents one data instance.

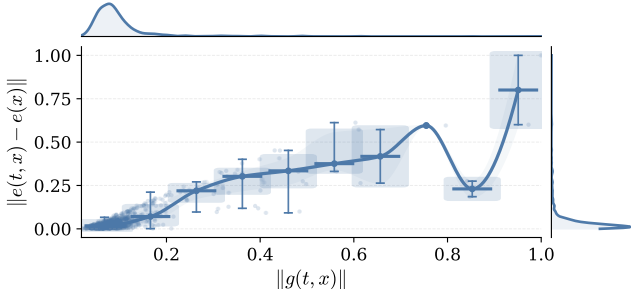


Figure 14. The variation of  $\|e(t, x) - e(x)\|$  with respect to  $\|g(t, x)\|$  of ICL, where each point represents one data instance. The Pearson correlation coefficient for the fitted points is 0.876.

text is not significantly constrained by the existing contexts, allowing the new context to still influence the reasoning outcome. (ii) In contrast, the norm of the contextual correction vector exhibits a decreasing trend, which indicates that the existing contexts can partially help resolve the query and thus reduce the model reliance on the new context.

#### D.5. Performance of Trained Predictor

The relative error of the trained predictor is shown in Table 8.

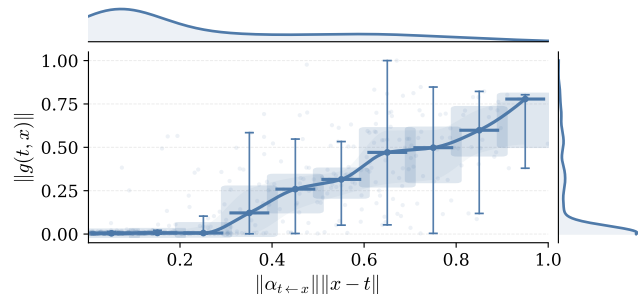


Figure 15. The variation of  $\|g(t, x)\|$  with respect to  $\alpha_{x-t} \|v_t - v_x\|$  of ICL, where each point represents one data instance. The Pearson correlation coefficient for the fitted points is 0.817.

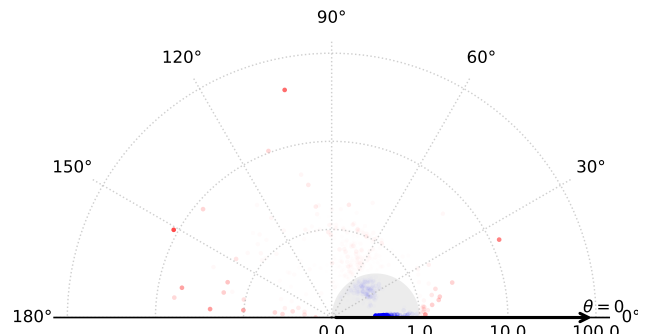


Figure 16. The variation of  $\|e(t, x)\| - \|e(x)\|$  with respect to  $g(t, x)$  of RAG, where each point represents one data instance.

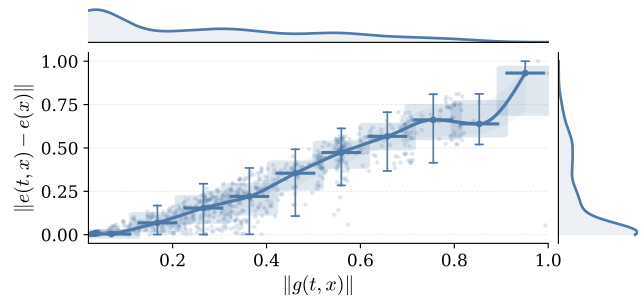


Figure 17. The variation of  $\|e(t, x) - e(x)\|$  with respect to  $\|g(t, x)\|$  of RAG, where each point represents one data instance. The Pearson correlation coefficient for the fitted points is 0.903.

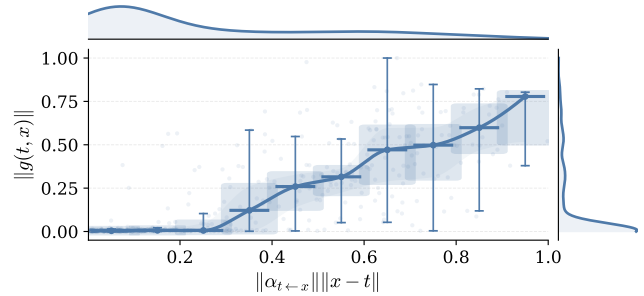


Figure 18. The variation of  $\|g(t, x)\|$  with respect to  $\alpha_{x-t} \|v_t - v_x\|$  of RAG, where each point represents one data instance. The Pearson correlation coefficient for the fitted points is 0.814.

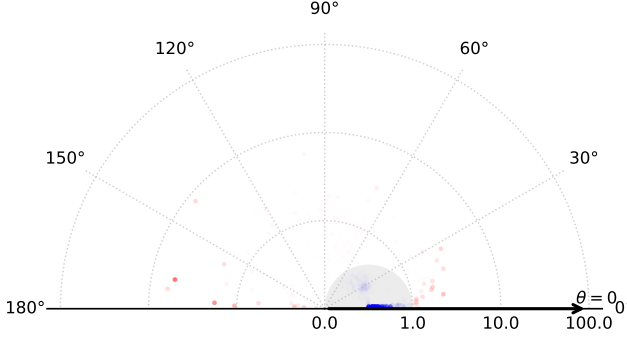


Figure 19. The variation of  $\|e(t, x)\| - \|e(x)\|$  with respect to  $g(t, x)$  of memory evolution, where each point represents one data instance.

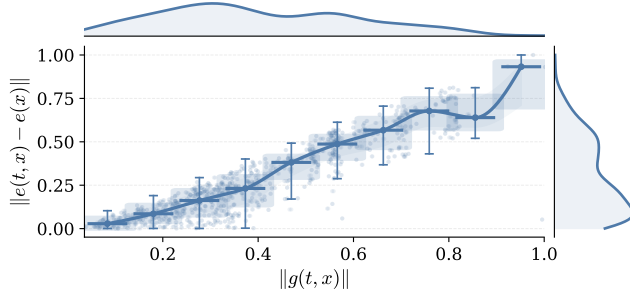


Figure 20. The variation of  $\|e(t, x)\| - \|e(x)\|$  with respect to  $\|g(t, x)\|$  of ICL, where each point represents one data instance of memory evolution. The Pearson correlation coefficient for the fitted points is 0.903.

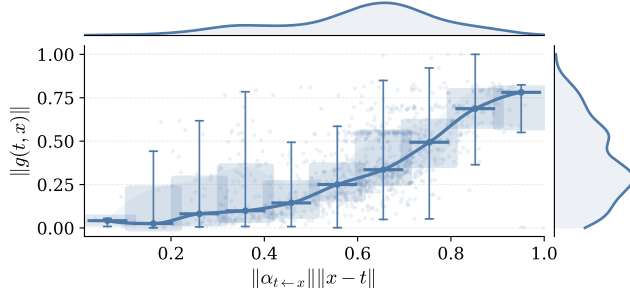


Figure 21. The variation of  $\|g(t, x)\|$  with respect to  $\alpha_{t-x}||v_t - v_x||$  of memory evolution, where each point represents one data instance. The Pearson correlation coefficient for the fitted points is 0.617.

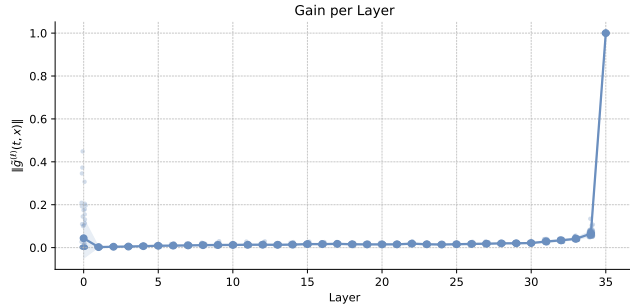


Figure 22. Variation of  $\|\tilde{g}^{(\ell)}(t, x)\|$  across all layers with respect to the layer index. To capture the trends across different models, we normalize the results separately for each setting.

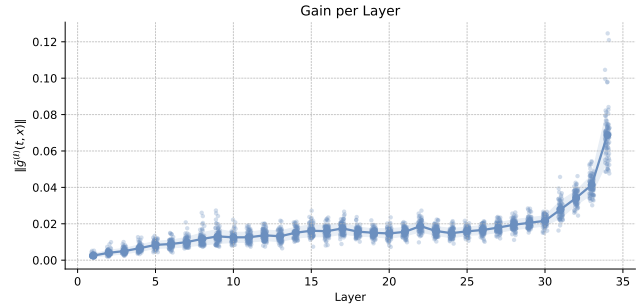


Figure 23. Variation of  $\|\tilde{g}^{(\ell)}(t, x)\|$  with respect to the layer index. The fitted Pearson correlation coefficient of the scatter points is 0.322. To capture the trends across different models, we normalize the results separately for each setting.

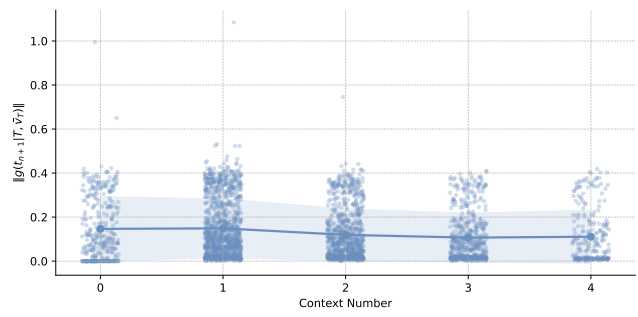


Figure 24. The norm of contextual correction vectors with different context numbers.

*Table 6.* The prompt of Thinker during memory evolution.

---

**Prompt of Thinker using Memory Evolution**

---

You are an expert meta-reasoning coach for AI agents.

You will receive a SINGLE data sample from an agent's past experience. This sample may include: a task description, the agent's thoughts/actions/observations, and whether the attempt succeeded or failed.

Your job is to distill this ONE example into ONE HIGH-LEVEL INSIGHT: a general rule or strategy that would be useful for similar future tasks.

===== INPUT SAMPLE =====

[Task description]

{TASK\_DESCRIPTION}

[Episode log / trajectory]

{EPISODE\_LOG}

Please now produce exactly ONE INSIGHT that:

- Is HIGH-LEVEL and GENERAL.
- It should be a reusable principle that could help on future, similar tasks.
- It should focus on better thinking and acting (e.g., how to search, plan, verify, explore).
  
- Is NOT tied to superficial details of this specific sample.
- Do NOT mention specific names, URLs, IDs, or exact numbers from the log unless they are essential to the principle.
- Do NOT describe the episode step-by-step.
- Do NOT say \In this trial..." or \In this example...". Instead, phrase it as \When solving tasks like this, you should...".
  
- Captures what the agent should DO DIFFERENTLY or KEEP DOING.
- If the attempt failed: focus on what change of strategy would most likely prevent this failure.
- If the attempt succeeded: focus on what strategy made it robust and should be repeated.

Output format (VERY IMPORTANT):

INSIGHT:

- <one single sentence (or two short sentences) stating the general rule>

Do NOT output anything else. No explanations, no justification, no bullet list of multiple rules.

Just the single \INSIGHT:" line as specified above.

---

Table 7. The case study of different relations between context vector and error. Cases are from MATH dataset using Llama-3.1-8B with ICL. Considering the space, we have removed information that is irrelevant to the reasoning process.

Type	Problem	Demonstration	Reasoning process
Error Reduction	Solve $4^x = 8$ and express $x$ as a common fraction.	Solve $2^8 = 4^x$ for $x$ .	I'll mirror the demonstration's strategy: rewrite both sides using the same base so I can compare exponents directly. Since $4 = 2^2$ and $8 = 2^3$ , we get $4^x = (2^2)^x = 2^{2x}$ . Then $2^{2x} = 2^3$ , so the exponents must match: $2x = 3$ . Therefore $x = \frac{3}{2}$ . Final answer: $\frac{3}{2}$ .
Mismatch Angle	You have 5 shirts, 6 pairs of pants, and 8 hats. How many outfits are possible if you choose one of each.	Solve $2^3 \cdot 3^x = 72$ for $x$ .	The demonstration looks like a template: rewrite numbers in prime powers and solve by matching exponents. I follow that template and start solving the demonstration-style equation $2^3 \cdot 3^x = 72$ : factor $72 = 2^3 \cdot 3^2$ , so $x = 2$ . I got pulled into the exponent-matching task from the demonstration and effectively answered the demonstration again, even though the question is actually about counting outfit combinations. Final answer: 2.
Overfit Norm	The sum of the first $N$ positive odd integers is 121. Find $N$ .	Find the smallest positive perfect cube that can be written as the sum of three consecutive integers.	In the demonstration, the move is to model a sum using three consecutive integers: $(n-1) + n + (n+1) = 3n$ . I reuse that pattern here and try to force 121 into the same shape: $121 \approx 3n$ . Since $121/3$ isn't an integer, I "fix" it by switching to the nearest multiple of 3: $120 = 39 + 40 + 41$ , so I take $n = 40$ . I over-focus on the demonstration's "three consecutive integers" structure and ignore the key phrase "first $N$ odd integers," which should drive a different solution. Final answer: 40.

Table 8. The relative error ( $\frac{|gold\_value - pred\_value|}{gold\_value}$ ) of the trained predictor under different settings.

Dataset	Method	Llama-3.1-8B	Qwen3-8B
MATH	ICL	33.8%	39.4%
	ME	38.3%	25.5%
CHAMP	RAG	27.0%	23.9%
	ME	34.4%	36.7%
TheoremQA	RAG	26.6%	26.0%
	ME	28.8%	29.5%
MMLU-Redux	ME	31.4%	33.4%
GPQA	ICL	34.4%	21.1%
	ME	37.4%	25.5%
NQ	ME	39.3%	33.5%
FinQA	ICL	25.2%	38.1%
	ME	38.1%	27.1%